

# EXCITATION OF THE 3.071 mm HYPERFINE LINE IN Li-LIKE $^{57}\text{Fe}$ IN ASTROPHYSICAL PLASMAS

NOELLA L. D'CRUZ AND CRAIG L. SARAZIN  
Department of Astronomy, University of Virginia,  
P.O. Box 3818, Charlottesville, VA 22903-0818;  
nld2n@virginia.edu, cls7i@virginia.edu

and

JACQUES DUBAU  
Observatoire de Paris, F 92195 Meudon Principal Cedex, France;  
dubau@delacroix.obspm.fr

*Accepted for publication by the Astrophysical Journal, 27 Jan 1998*

## ABSTRACT

As noted first by Sunyaev & Churazov (1984), the 3.071 mm hyperfine line from  $^{57}\text{Fe}^{+23}$  might be observable in astrophysical plasmas. We assess the atomic processes which might contribute to the excitation of this line. The distorted wave approximation was used to compute the direct electron collision strength between the two hyperfine sublevels of the ground configuration; it was found to be small. Proton collisional excitation was calculated and found to be negligible. We determine the rate of line excitation by electron collisional excitation of more highly excited levels, followed by radiative cascades. The branching ratios for hyperfine sublevels for allowed radiative decays and electron collisional excitation or de-excitation are derived. We show that the dominant line excitation process is electron collisional excitation of the 2p levels followed by radiative decay, as first suggested by Sunyaev & Churazov (1984). We calculate an effective collision strength for excitation of the hyperfine line, including all of these effects and correcting for resonances. Because the hyperfine line is near the peak in the Cosmic Microwave Background Radiation spectrum, induced radiative processes are also very important. The effect of background radiation on the level populations and line excitation is determined.

We determine the intensity of the hyperfine line from an isothermal, coronal plasma in collisional ionization equilibrium. Because of the variation in the ionization fraction of  $\text{Fe}^{+23}$ , the emissivity peaks at a temperature of about  $1.8 \times 10^7$  K. We have also derived the hyperfine line luminosity emitted by a coronal plasma

cooling isobarically due to its own radiation. Comparisons of the hyperfine line to other lines emitted by the same ion,  $\text{Fe}^{+23}$ , are shown to be useful for deriving the isotopic fraction of  $^{57}\text{Fe}$ . We calculate the ratios of the hyperfine line to the 2s–2p EUV lines at 192 Å and 255 Å, and the 2s–3p X-ray doublet at 10.6 Å.

*Subject headings:* atomic data — atomic processes — hyperfine structure — line formation — radiative transfer — radio lines: general

## 1. INTRODUCTION

Astrophysically, the most important and well studied atom exhibiting hyperfine structure is the neutral hydrogen atom. Its hyperfine transition at 21 cm has been observed for many years both in emission and absorption in the gas in our Galaxy and other galaxies, and has provided information on the velocity structure of these systems (see Dickey & Lockman 1990 for a review). Besides this line, hyperfine emission from  $^3\text{He}$  has also been observed in our Galaxy in planetary nebulae (Balser et al. 1997) and H II regions (Rood et al. 1995). There have also been a number of searches for the 92 cm hyperfine line in deuterium (e.g., Lubowich, Anantharamiah, & Pasachoff 1989). In this paper, we are concerned with another atomic hyperfine transition which could possibly be of astrophysical interest — the 3.071 mm line (Shabaeva & Shabaev 1992) in Li-like  $^{57}\text{Fe}$ . As originally suggested by Sunyaev & Churazov (1984), it is potentially observable in a variety of astrophysical systems containing very diffuse, hot plasma ( $T \sim 10^7$  K), including clusters of galaxies, elliptical galaxies, hot interstellar gas in our own Galaxy, and supernova remnants. In a related paper, we calculate the line intensities expected from cooling flow and non-cooling flow clusters of galaxies (D’Cruz & Sarazin 1997; hereafter Paper II).

In the hot plasmas which would emit the  $^{57}\text{Fe}$  hyperfine line, the dominant radiation is X-ray line and continuum emission. However, observations of the  $^{57}\text{Fe}$  hyperfine line might have several advantages compared to X-ray line observations of the same plasma. First, the atmospheric absorption at 3.071 mm is low enough to allow ground based observations with large radio telescopes. Second, the spectral resolution of radio detectors vastly exceeds that of all existing or planned astrophysical X-ray spectrometers. Thus, observations of the 3.071 mm line could be used to determine the velocity field (bulk motions, turbulence, and thermal velocities) in the hot gas in clusters of galaxies and supernova remnants. Third, the detection of this  $^{57}\text{Fe}$  hyperfine line would allow the abundance of this isotope to be determined relative to the more common  $^{56}\text{Fe}$  isotope. Since these two isotopes are produced by different nuclear processes, this would provide a powerful constraint of nucleosynthesis in supernova remnants and on the chemical history of the intracluster gas. In this regard, the most direct measure of the isotope ratio comes from the ratio of the radio line from  $^{57}\text{Fe}$  to the EUV and X-ray lines from the same ion, Fe XXIV.

The 3.071 mm hyperfine line arises from the ground level ( $1s^2 2s \ ^2S_{1/2}$ ) of  $^{57}\text{Fe}$  XXIV. The nuclear spin of the  $^{57}\text{Fe}$  isotope is  $I = 1/2$ , so the total angular momentum is  $F = 0$  or 1. We denote the lower hyperfine sublevel ( $F = 0$ ) with the subscript  $l$ , and the upper hyperfine sublevel ( $F = 1$ ) with the subscript  $u$ . The statistical weights of the hyperfine sublevels are  $g_l = 1$  and  $g_u = 3$ . The rate of spontaneous radiative decay of the upper sublevel is  $A_{ul} = 9.4 \times 10^{-10} \text{ s}^{-1}$  (Sunyaev & Churazov 1984).

In this paper, we evaluate the atomic processes that lead to the production of the hyperfine line in Li-like  $^{57}\text{Fe}$ . We consider direct electron collisional excitation (§ 2.1), proton collisional excitation (§ 2.2), indirect excitation to higher levels followed by radiative cascades (§ 3), and stimulated radiative processes due to the Cosmic Microwave Background Radiation (CMBR) field (§ 4). We present new calculations for the rate of direct electron excitation of the upper hyperfine line (§ 2.1), and for indirect excitation of the 2p sublevels in the same ion, followed by cascade (§ 3.3). We derive the branching ratios for radiative and collisional transitions between the hyperfine sublevels of  $^{57}\text{Fe}$  XXIV (§§ 3.1, 3.2). A total effective collision strength for exciting the line is given in § 3.5. The rate of excitation due resonant scattering of UV and X-ray lines (optical pumping) is discussed in § 3.6. The radiative transfer of the line and of the CMBR is discussed in § 5. The resulting line intensities in a few simple situations are given in § 6, where they are also compared to the line intensities for several EUV and X-ray lines from Fe XXIV. Finally, the results are summarized in § 7. These excitation rates are used to predict the fluxes of this line from clusters in Paper II.

## 2. DIRECT COLLISIONAL EXCITATION

### 2.1. Direct Electron Collisional Excitation

The cross-section for direct electron collisional excitation of the excited hyperfine sublevel is  $\sigma(E) = [\Omega_{lu}/(g_l E)]\pi a_o^2$ , where  $E$  is the colliding electron kinetic energy (in Ryd),  $a_o$  is the Bohr radius, and  $\Omega_{lu}$  is the collision strength. The direct electron collision strength between the hyperfine sublevels was calculated using the distorted wave approximation code developed by Eissner & Seaton (1972). For the Li-like target wavefunctions, the SUPERSTRUCTURE code was used. At the temperatures of interest, the excitation energy of the upper hyperfine sublevel,  $\Delta E_{lu}$ , is very small compared to the kinetic energy of the colliding electron, and the collision is therefore assumed to be elastic.

The reactance matrix elements corresponding to elastic collisions within the  $1s^2 2s$  configuration in LS coupling have been converted to hyperfine structure coupling with  $2 \times 4$  6-j symbols. This method of recoupling is similar to the method used for fine structure reactance matrices (e.g., see the JAJOM program [Saraph 1978]). To avoid confusion, we use the same notation as Saraph (1978). Let  $L_i$ ,  $S_i$ , and  $J_i$  denote the orbital, spin, and total electronic angular momenta, respectively, of the Li-like target ion. Let  $l_i$  and  $s_i = 1/2$  be the orbital and spin angular momenta of the electronic projectile. When we include the nuclear spin  $I = 1/2$ , the total angular momentum of the target ion becomes  $F_i$ , where  $\mathbf{F}_i = \mathbf{J}_i + \mathbf{I}$ . We define the following intermediate couplings:  $\mathbf{K}_i = \mathbf{J}_i + \mathbf{l}_i$  and  $\mathbf{G}_i = \mathbf{F}_i + \mathbf{l}_i$ . The subscripts  $i$  corresponds to any collision channel, while we use  $j$  for the initial channel. During

the collision, the interaction responsible for the transition is the electron-electron electrostatic interaction. The conservation relations for this interaction are  $\mathbf{L} = \mathbf{L}_j + \mathbf{l}_j = \mathbf{L}_i + \mathbf{l}_i$ ,  $\mathbf{S} = \mathbf{S}_j + \mathbf{s}_j = \mathbf{S}_i + \mathbf{s}_i$ , and  $p = p_j = p_i$ , where  $p$  is the parity of the system. Thus, the total electronic angular momentum of the (target + projectile) system,  $\mathbf{J} = \mathbf{L} + \mathbf{S}$ , as well as the total angular momentum including the nuclear spin,  $\mathbf{F} = \mathbf{I} + \mathbf{J}$ , are conserved. The other quantum numbers necessary to define uniquely the target state will be denoted by  $\Gamma_i$ . Using Racah algebra and recoupling of the angular momenta, it is possible to obtain the reactance matrix elements between  $Fp$  channels from the ones between  $SLp$  channels as

$$R^{Fp}(\Gamma_i S_i L_i J_i F_i l_i G_i; \Gamma_j S_j L_j J_j F_j l_j G_j) = \sum_{\substack{SLJ \\ \kappa_i \kappa_j}} C(SLJK_i, S_i L_i J_i F_i l_i G_i) \\ \times R^{SLp}(\Gamma_i S_i L_i l_i; \Gamma_j S_j L_j l_j) C(SLJK_j, S_j L_j J_j F_j l_j G_j), \quad (1)$$

where

$$C(SLJK_i, S_i L_i J_i l_i G_i) = (-1)^a (2K_i + 1) \\ \times [(2S + 1)(2L + 1)(2J_i + 1)(2J + 1)(2G_i + 1)(2F_i + 1)]^{1/2} \\ \times \begin{Bmatrix} I & J_i & F_i \\ l_i & G_i & K_i \end{Bmatrix} \begin{Bmatrix} S_i & L_i & J_i \\ l_i & K_i & L \end{Bmatrix} \begin{Bmatrix} I & K_i & G_i \\ 1/2 & F & J \end{Bmatrix} \begin{Bmatrix} L & S_i & K_i \\ 1/2 & J & S \end{Bmatrix}. \quad (2)$$

The phase factor is  $a = S_i - J_i + K_i - I - F_i - G_i - S - J$ . The collision strengths are obtained directly from the reactance matrices (Saraph 1978).

Figure 1 shows the resulting collision strength for direct electron excitation as function of the kinetic energy of the electron. Note that the collision strength is quite small ( $\Omega_{lu} \approx 10^{-3}$ ) at the energies of interest ( $E \approx 10^2$  Ryd). Direct collisional excitation is weak, in part, because the transition is radiatively forbidden, and the forbidden transition rates drop off rapidly at energies which greatly exceed the excitation energy. As we shall see below, the small collision strength for direct excitation indicates that this is not a very significant process at temperatures of interest. While working on this paper, we received a preprint from Sampson & Zhang (1997) which presented relativistic distorted wave calculations of the collision strength for the same transition. The Sampson & Zhang collision strength is shown as a dashed curve in Figure 1. These calculations are in good agreement with our calculations; the Sampson & Zhang collision strengths are about 7% lower than ours.

The rate of electron collisions which directly excite the hyperfine line per unit volume is  $n_l n_e q_{lu}^{\text{dir}}$ , where  $n_e$  is the electron number density and  $n_l$  is the number density of Li-like  $^{57}\text{Fe}$  in the lower hyperfine sublevel. The rate coefficient is

$$q_{lu}^{\text{dir}} = \frac{8.629 \times 10^{-6} \bar{\Omega}_{lu}(T)}{g_l T^{1/2}} \exp\left(\frac{-\Delta E_{lu}}{kT}\right) \text{ cm}^3 \text{ s}^{-1}. \quad (3)$$

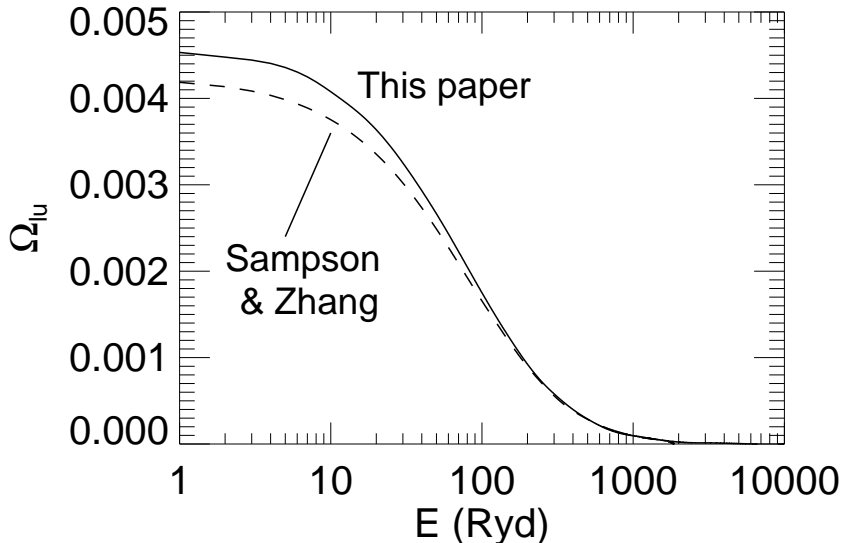


Fig. 1.— strength for direct electron excitation of the hyperfine line as a function of the electron kinetic energy in Rydbergs. The solid curve gives our result, while the dashed line is from Sampson & Zhang (1997).

Here,  $\bar{\Omega}_{lu}(T) \equiv \int_0^\infty \Omega_{lu}(E) \exp(-E/kT) d(E/kT)$ , is the thermally-averaged direct collision strength. The value of  $\bar{\Omega}_{lu}(T)$  as a function of temperature is shown in Figure 2, which is based on the values in Figure 1, for both our calculations and the Sampson & Zhang work. The rate coefficient for de-excitation is related to equation (3) by detailed balance.

## 2.2. Direct Proton Collisional Excitation

Often, proton collisions contribute significantly to the excitation of low-lying energy levels at high temperatures ( $kT \gg \Delta E$ ). This condition clearly applies to the hyperfine sublevels under consideration, but not so strongly to other excited levels in the Fe XXIV ion. Protons are not important for exciting higher levels in Fe XXIV, because they move slower than electrons, undergo Coulomb repulsion, and do not participate in exchange reactions.

The theory of proton collisional excitation was first developed by Seaton (1964), who adapted the theory by Alder et al. (1956) for nuclear Coulomb excitations. Seaton (1964) and Bely & Faucher (1970) used this formalism to calculate the rate of proton collisional excitation of fine structure levels. This theory can also be applied to the excitation of hyperfine transitions. Kastner (1977) and Kastner & Bhatia (1979) give detailed expressions for proton excitation rates based on the theory of Seaton (1964) and Bely & Faucher (1970).

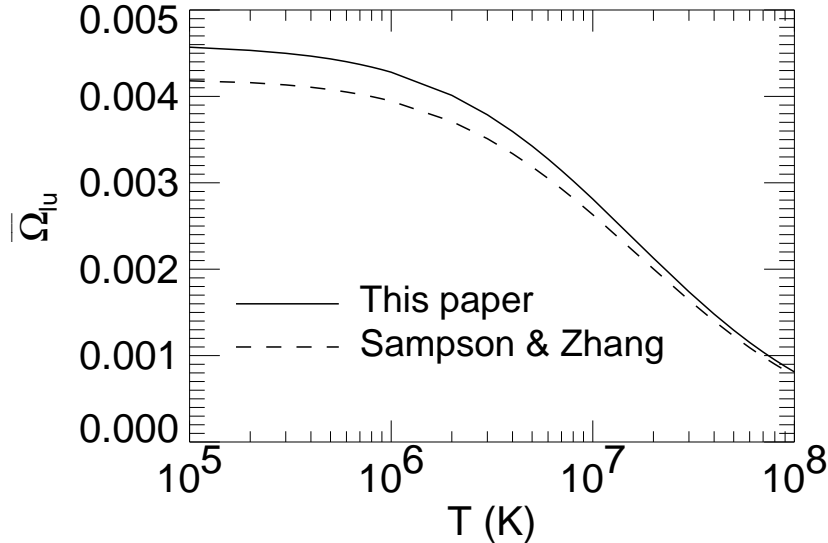


Fig. 2.— Thermally-averaged collision strength for direct electron excitation of the hyperfine line as a function of temperature. The solid curve gives our result, while the dashed line is from Sampson & Zhang (1997).

We applied these expressions to calculate the direct proton excitation of the hyperfine sublevels of the Li-like  $^{57}\text{Fe}$  ion. According to this theory, proton excitations of the fine and hyperfine structure sublevels occur primarily through interactions with the electric quadrupole moment of the ion. For the Li-like ions, the outermost free electron is in the 2s state. Of course, this state is spherically symmetric, and as such has no quadrupole moment. Hence, the dominant term in the rate coefficient for proton excitation is zero.

The next most important term in proton collisional excitation is due to the magnetic dipole interaction. In general, magnetic dipole cross-sections are smaller than electric quadrupole cross-sections by a factor of about  $10^{-5}$  (Alder et al. 1956; Bahcall & Wolf 1968). To check the importance of magnetic dipole excitation rates due to protons, we compared the rate coefficients for this process with that due to electron collisions. The magnetic dipole excitation rates were several orders of magnitude smaller than the electron collision rates. Hence, proton collisions can be neglected.

### 3. INDIRECT COLLISIONAL EXCITATION AND CASCADE

The most important process for exciting the hyperfine line turns out to be electronic collisional excitation to a more highly excited state, followed by radiative cascade to the

excited hyperfine sublevel. We refer to this process as “indirect collisional excitation.” The rate coefficient for excitation of the upper hyperfine sublevel due to excitations of higher levels followed by cascades is given by

$$q_{lu}^{\text{indir}} = \frac{8.629 \times 10^{-6}}{g_l T^{1/2}} \sum_{k>u} C(k, u) \bar{\Omega}_{lk}(T) \exp\left(\frac{-\Delta E_{lk}}{kT}\right) \text{ cm}^3 \text{ s}^{-1}, \quad (4)$$

where the cascade matrix  $C(k, u)$  gives the probability that the radiative decay of level  $k$  will eventually lead to the excitation of the level  $u$ .

In this section, we derive the branching ratios for radiative decays, calculate in detail indirect excitation of the hyperfine line through the  $1s^2 2p$  configuration, give an approximate calculation of the rate of indirect excitations through more highly excited levels, and determine an effective collision strength which gives the total rate of collisional excitation of the hyperfine line.

### 3.1. Radiative Cascades

With the exception of the upper hyperfine sublevel in the ground configuration of  $^{57}\text{Fe}$  XXIV, all of the excited sublevels have allowed radiative decays. Here, we give the branching ratios among the allowed decays between the hyperfine sublevels. We assume LS coupling. Consider the allowed decays between the an upper level with total electron spin  $S$ , total electron orbital angular momentum  $L$ , and total electron angular momentum  $J$ , and a lower level with quantum numbers  $S'$ ,  $L'$ , and  $J'$ . Let the nuclear angular momentum be  $I$ . Let  $A(SLJ, S'L'J')$  be the radiative decay rate between the two levels, averaging over the hyperfine structure (e.g., the value normally given in tables of atomic data). Let  $F$  and  $F'$  be two hyperfine sublevels of the upper and lower levels, respectively. Assume that the hyperfine splittings are small, so that all of the hyperfine transitions have essentially the same wavelength. Then, irreducible tensor analysis can be used to derive the radiative decay rate between the hyperfine sublevels, which is given in terms of a 6-j symbol as

$$A(SLJF, S'L'J'F') = A(SLJ, S'L'J')(2F' + 1)(2J + 1) \left\{ \begin{array}{ccc} J' & J & 1 \\ F & F' & I \end{array} \right\}^2. \quad (5)$$

The nuclear spin of  $^{57}\text{Fe}$  is  $I = 1/2$ . The total decay rate for any given hyperfine sublevel to all of the hyperfine sublevels of a lower level is then

$$\sum_{F'} A(SLJF, S'L'J'F') = A(SLJ, S'L'J'), \quad (6)$$



where this follows from the orthonormality relation for the 6-j symbols. Thus, the total rates of decay of all of the upper hyperfine levels are identical and equal to the rate if the hyperfine structure is not resolved.

Let  $P(nJF, n'J'F')$  be the probability that the excited hyperfine sublevel  $nJF$  decays directly to the hyperfine sublevel  $n'J'F'$ , rather than any other level. Here,  $n$  and  $n'$  represents any other quantum numbers which label the levels. Thus,

$$P(nJF, n'J'F') \equiv \frac{A(nJF, n'J'F')}{\sum_{n'', J'', F''} A(nJF, n''J''F'')}. \quad (7)$$

If one substitutes equation (6) for the decay rate, and simplifies the denominator using the orthonormality relation for 6-j symbols, the decay probability becomes

$$P(nJF, n'J'F') = P(nJ, n'J')(2F' + 1)(2J + 1) \left\{ \begin{matrix} J' & J & 1 \\ F & F' & I \end{matrix} \right\}^2. \quad (8)$$

Here,  $P(nJ, n'J')$  is the decay probability if the fine structure is not resolved,

$$P(nJ, n'J') \equiv \frac{A(nJ, n'J')}{\sum_{n'', J''} A(nJ, n''J'')}. \quad (9)$$

A very useful quantity in describing indirect collisional excitation and cascades is the cascade matrix  $C(nJF, n'J'F')$ , which is defined as the probability that an excitation of the  $nJF$  hyperfine sublevel leads to a population of the  $n'J'F'$  sublevel by all possible radiative cascade routes. Then, if one starts with the obvious result that  $C(nJF, nJF) = 1$ , one can determine the cascade matrix recursively from the relationship

$$C(nJF, n'J'F') = \sum_{\substack{n, J, F \\ (n'', J'', F'') > (n', J', F')}} C(nJF, n''J''F'') P(n''J''F'', n'J'F'), \quad (10)$$

where the sum extends to all levels above the  $n'J'F'$  sublevel, up to and including the  $nJF$  sublevel. If the upper level  $nJ$  is far above the lower level  $n'J'$ , and there are many intervening levels with allowed decays, and complex cascades dominate the cascade matrix, so that  $C(nJF, n'J'F') \gg P(nJF, n'J'F')$  and  $P(nJF, n'J'F') \ll 1$ , then equation (10) has the approximate solution

$$C(nJF, n'J'F') \approx C(nJ, n'J') \frac{(2F' + 1)}{(2F + 1)} \frac{(2J + 1)}{(2J' + 1)}, \quad (11)$$

where  $C(nJ, n'J')$  is the cascade matrix if the hyperfine structure is not resolved. Thus, complex cascades lead to the populations of hyperfine sublevels  $F'$  in proportion to their statistical weights.

A similar result occurs if the upper hyperfine sublevels  $F$  are populated in proportion to their statistical weights. Then, the average decay probability to the lower hyperfine sublevels  $F'$  is

$$\langle P(nJ, n'J'F') \rangle \equiv \sum_F \frac{(2F+1)}{(2J+1)(2I+1)} P(nJF, n'J'F') = \frac{(2F'+1)}{(2J'+1)(2I+1)} P(nJ, n'J'). \quad (12)$$

Thus, the lower hyperfine sublevels  $F'$  are again populated in proportion to their statistical weights.

The only levels with allowed decays to the ground configuration in Fe XXIV are  $1s^2 np \ ^2P_J$  levels with  $J = 1/2$  or  $3/2$ . The decay probabilities for these hyperfine radiative transitions are listed in Table 1.

Table 1: Hyperfine Radiative Decay Probabilities  $P(JF, J'F')$

Lower Level	Upper Level			
	$J = 1/2$		$J = 3/2$	
	$F = 0$	$F = 1$	$F = 1$	$F = 2$
$F' = 0$	0	1/3	2/3	0
$F' = 1$	1	2/3	1/3	1

### 3.2. Hyperfine Branching Ratios for Electron Collisional Excitation

Collision strengths are available in the literature for excitations to excited levels in Fe XXIV, although these collisional rates average over the hyperfine structure in  $^{57}\text{Fe}$  XXIV. Thus, it is not generally necessary to calculate all of the collision rates anew. Instead, what is needed are the branching ratios for the collisional rates among the hyperfine sublevels. These branching ratios can be determined using irreducible tensor analysis, assuming that the hyperfine structure has a negligible effect on the collision rates. The interaction Hamiltonian between the bound electron and the colliding free electron can be expanded as a power series with terms  $(r_{<}^\lambda/r_{>}^{\lambda+1})$ , where  $\lambda$  is the index of the series, and  $r_{<}$  and  $r_{>}$  are the smaller and larger of the radii of the two interacting electrons. The interactions are further divided into direct interactions (D) in which the bound and free electrons retain their identities, and exchange interactions (E) in which they exchange identities.

For an alkali ion, such as the Li-like system, only the valence electron is strongly affected during the collision. Configuration interactions are negligible between target terms, and only

one  $\lambda$  term contributes to the direct interaction for transitions from the 2s configuration. We can therefore simplify the Racah algebra and reduce the 8 6-j symbols which arise when equation (2) is squared to only 2 6-j symbols. For either direct or exchange reactions, the collision strength for a transition between the hyperfine sublevels is given approximately by

$$\Omega(F, F') = \Omega(J, J')(2F + 1)(2F' + 1) \left\{ \begin{array}{ccc} J' & J & \lambda \\ F & F' & I \end{array} \right\}^2, \quad (13)$$

where  $\Omega(J, J')$  is the collision strength between the fine structure levels, ignoring the hyperfine structure and nuclear spin. An equivalent result has been given by Sampson & Zhang (1997), based on jj coupling. If LS coupling is assumed and the fine structure splitting are also small, then this branching relationship can be extended to include the fine structure in direct interactions as

$$\begin{aligned} \Omega^D(JF, J'F') &= \Omega^D(LS, L'S) \frac{(2J + 1)(2J' + 1)(2F + 1)(2F' + 1)}{(2S + 1)} \\ &\times \left\{ \begin{array}{ccc} L' & L & \lambda \\ J & J' & S \end{array} \right\}^2 \left\{ \begin{array}{ccc} J' & J & \lambda \\ F & F' & I \end{array} \right\}^2. \end{aligned} \quad (14)$$

Here,  $\Omega^D(LS, L'S)$  is the direct collision strength between the two terms, ignoring the fine structure. For direct interactions, the electron spin  $S$  is unchanged.

### 3.3. Indirect Excitation Through 2p Sublevels

In the compilation of collision strengths for Fe XXIV in Gallagher & Pradhan (1985), the largest excitation rates from the 2s ground configuration are to the levels in the low lying 2p configuration. Thus, we treat the 2p sublevels in detail because their collision strengths dominate the excitation of the hyperfine line. These sublevels are shown schematically in Figure 3. The allowed radiative decays and collisional excitation and de-excitation processes are indicated, along with the radiative and collisional branching ratios.

For each of the transitions between 2s and 2p hyperfine sublevels, the collision strength and radiative decay rate (for allowed transitions) were calculated, using the same distorted wave method and recoupling scheme discussed in § 2.1. In Figure 4, we illustrate these values by giving the collision strengths for transitions between the ground hyperfine 2s  $F = 0$  sublevels and the excited 2p hyperfine sublevels. The values are given as a function of the incident electron energy (in Rydbergs) for low energy collision ( $E \leq 50$  Ryd). These results illustrate several points about the collisional excitation.

First, even at these low energies, the collisional excitation is dominated by allowed transitions. Collisional excitations and de-excitations between the 2s  $^2\text{S}_{1/2}$   $F = 0$  hyperfine

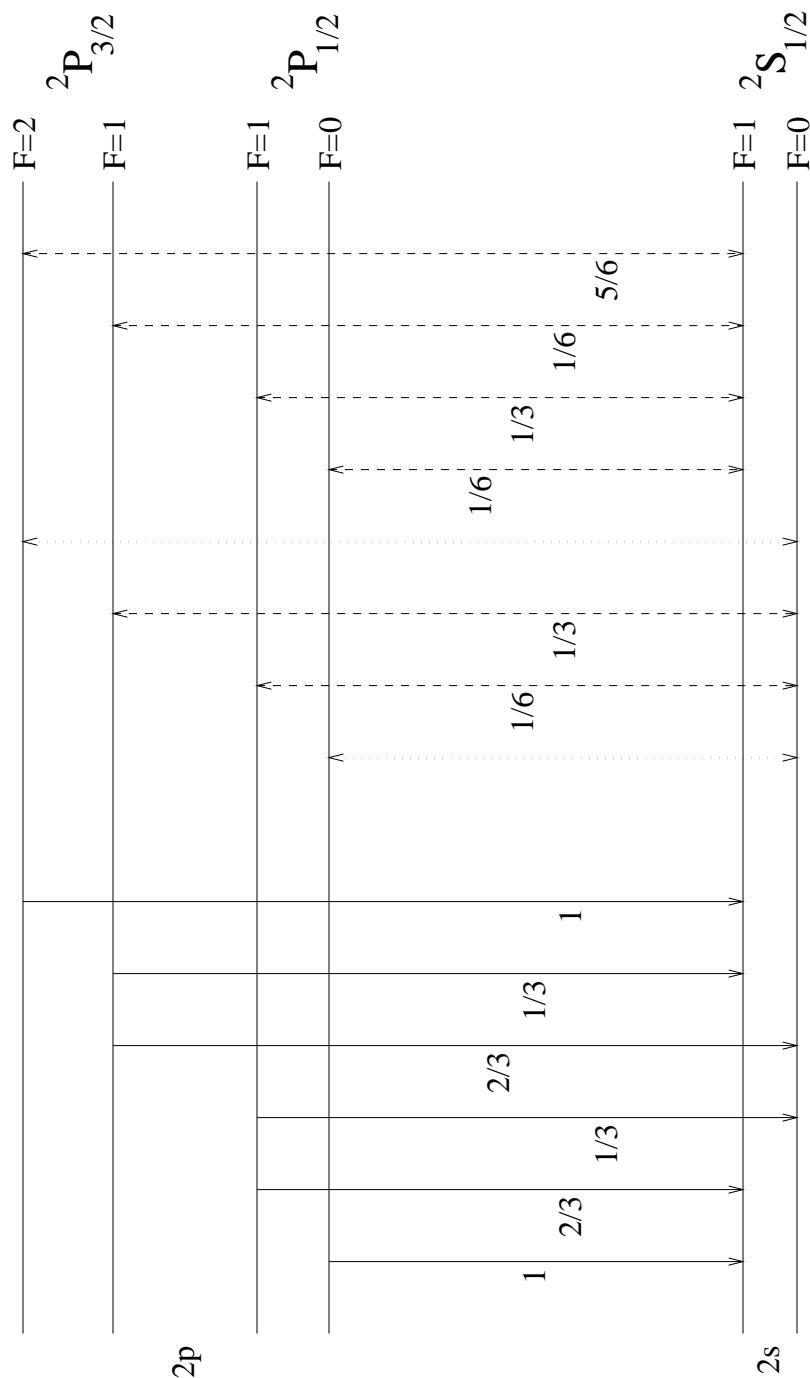


Fig. 3.— A schematic energy level diagram of the 2s and 2p hyperfine levels for  $^{57}\text{Fe}$  XXIV. The energies are not shown to scale. The vertical solid lines on the left show the allowed radiative decays, and the numbers give the branching ratios as defined in Table 1. The vertical lines at the right are the collisional transitions. The dashed lines give the allowed transitions, and the numbers give the branching ratios as defined in Table 2. The dotted lines are the weaker forbidden transitions.

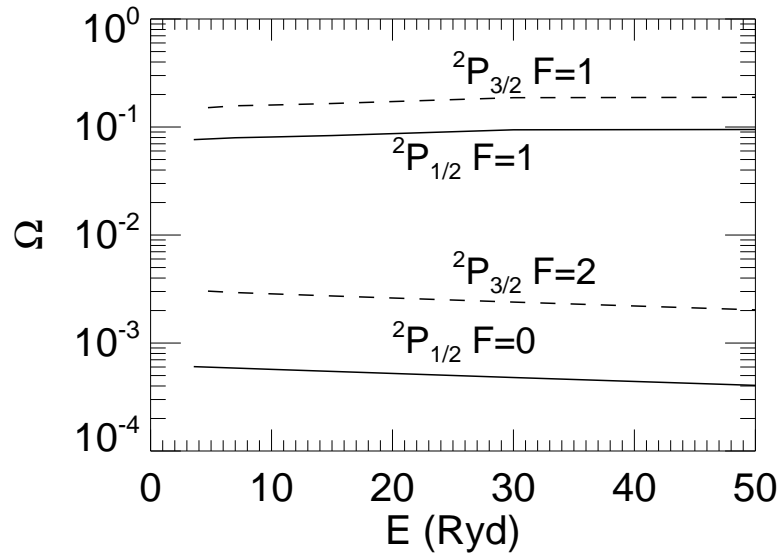


Fig. 4.— Collision strength versus incident electron energy (in Rydbergs) for electron collisions between the ground hyperfine  $2s$   $F = 0$  levels and the excited  $2p$  hyperfine levels of  $^{57}\text{Fe}$  XXIV.

sublevel and the  $2p$   $^2P_{1/2}$   $F = 0$  or  $^2P_{3/2}$   $F = 2$  hyperfine sublevels are forbidden. In Figure 4, the rates for these forbidden transitions are at least a factor of 20 smaller than the rates for the allowed transitions from the ground  $2s$   $^2S_{1/2}$   $F = 0$  hyperfine sublevel to the  $2p$   $^2P_{1/2}$   $F = 1$  or  $^2P_{3/2}$   $F = 1$  sublevels. When one goes to even higher energies, the allowed transitions dominate even more strongly. In collisional ionization equilibrium, the excitation of the  $^{57}\text{Fe}$  XXIV line should occur mainly at  $E \approx 10^2$  Ryd or  $T \approx 2 \times 10^7$  K (§ 6). This is considerably greater than the threshold for the excitation of the  $2p$   $^2P_{1/2}$  or  $2p$   $^2P_{3/2}$  levels. Thus, one expects that collisional excitation will be dominated by radiatively allowed transitions. As a result of radiative excitation of the hyperfine ground levels by the cosmic microwave background radiation, the populations of the two hyperfine ground sublevels are expected to be comparable (§ 4). Now, all of the  $2p$  hyperfine sublevels have allowed transitions from either one or both of the ground hyperfine sublevels. Thus, the indirect excitation of the  $^{57}\text{Fe}$  XXIV line through the  $2p$  sublevels will be dominated by allowed electron collisional excitations.

For these allowed electron collisional excitations, the branching ratios are given by equations (13) or (14) with  $\lambda = 1$ . Alternatively, the branching ratios can be found by application of the Van Regemorter (1962) effective Gaunt factor approximation with the radiative branching ratios in Table 1. The branching ratios  $\Omega(F, F')/\Omega(2s, 2p)$  for the collision strengths for the allowed  $2s$  to  $2p$  transitions are given in Table 2, where  $\Omega(2s, 2p)$  is the total collision strength between the two terms (ignoring the nuclear spin). The branching

ratios for allowed collisional excitations are also shown in the left half of Figure 3.

Table 2: Hyperfine Allowed Collisional Branching Ratio  $\Omega(F, F')/\Omega(2s, 2p)$

Lower Level	Upper Level			
	$J = 1/2$		$J = 3/2$	
	$F' = 0$	$F' = 1$	$F' = 1$	$F' = 2$
$F = 0$	0	1/6	1/3	0
$F = 1$	1/6	1/3	1/6	5/6

Second, the collisional excitations and de-excitations between the  $2s\ ^2S_{1/2}\ F = 0$  hyperfine sublevel and the  $2p\ ^2P_{1/2}\ F = 0$  or  $^2P_{3/2}\ F = 2$  hyperfine sublevels are forbidden. As noted above, the collisions have a significantly reduced rate relative to the allowed collision. For forbidden transitions between the singlet  $2s\ F = 0$  hyperfine sublevel and the other sublevels, the collision strength is proportional to the statistical weight of the upper sublevel, so that  $\Omega(2s\ F = 0, 2p\ F = 2)/\Omega(2s\ F = 0, 2p\ F = 0) = 5$ , as shown in Figures 4.

Third, the collisional excitation rates based on our calculations of the collision strength between individual hyperfine sublevels are in excellent agreement ( $\lesssim 7\%$ ) with the values determined by applying the collisional branching ratios (Table 2 or eq. (13)) to the total collision strengths from Hayes (1979). The values in Hayes are the ones used to calculate EUV and X-ray lines from the same ion; as discussed in § 6, these EUV and X-ray lines can be used with the hyperfine line to determine the abundance of  $^{57}\text{Fe}$  accurately. For consistency with with EUV and X-ray analyses of the same plasma, we have adapted the Hayes (1979) collision strengths together with the relevant branching ratios.

### 3.4. Indirect Excitation Through Higher Levels

The collision strengths from the ground configuration to more excited configurations than 2p were obtained from the critical compilation of Gallagher & Pradhan (1985). For most of these transitions, the data come from Hayes (1979). The rest are from Mann (1983). The standard fitting formulae for collision strengths given in Clark et al. (1982) were used to fit the variation of each collision strength with temperature. The collision strength branching ratios of equation (13) were used to partition the collisional excitations among the initial and final hyperfine sublevels. Equations (5) and (10) were used to determine the cascade matrix from the hyperfine sublevels. However, it is worth noting that the collision strengths to higher levels are all at least 30 times smaller than the collision strengths to the 2p levels,

so their contribution is small. Sunyaev & Churazov (1984) first suggested that the dominant line excitation process for this hyperfine line is electron collisional excitation of the 2p levels.

Collisional ionization and recombination also make a small contribution to the overall excitation rate for the hyperfine sublevels. We assume that these processes populate the hyperfine sublevels in proportion to their statistical weights. Note that the cascade matrix among hyperfine sublevels will preserve such a distribution if it is established in the upper sublevels (eq. 12).

### 3.5. *Effective Collision Strength and Resonances*

The collision strengths for direct excitation and indirect excitation of the hyperfine line can be combined to give a single effective collision strength for the transition. By combining equations (3) and (4), one finds

$$\bar{\Omega}_{lu}^{\text{eff}} = \bar{\Omega}_{lu} + \sum_{k>u} \bar{\Omega}_{lk}(T) C(k, u) \exp\left(\frac{-\Delta E_{uk}}{kT}\right). \quad (15)$$

The distorted wave method used to determine the direct collision strength did not include the effect of resonances on the collision rate. Resonances are less important when the incident energy greatly exceeds the excitation energy of the transition. Thus, we do not expect resonances to strongly affect the collisional excitation of the hyperfine line. In collisional excitation through a resonance, the incident free electron and a bound electron form a bound autoionizing state, which autoionizes leaving one bound electron in an excited level. An approximation to the resonance excitation process is to treat each resonance as a direct collisional excitation in which the incoming electron has an energy which is lower than the threshold  $\Delta E_{lk}$  for the excitation (Seaton 1966; Petrini 1970; Mason 1975). The probabilities for the various decay channels of the autoionizing state in the resonance are given by the branching ratios for radiative decay. These same radiative decay probabilities are included in the cascade matrix  $C(k, u)$ . If the resonance structure is assumed to extend down to the level  $u$ , the combined effect of resonances and cascades is given approximately by equation (4), with the excitation energy of the highly excited state replaced by  $\Delta E_{lu}$  (Mason 1975). Thus, we can include resonances approximately by replacing the effective collision strength in equation (15) with

$$\bar{\Omega}_{lu}^{\text{eff}} = \bar{\Omega}_{lu} + \sum_{k>u} \bar{\Omega}_{lk}(T) C(k, u). \quad (16)$$

We use this expression to determine the rate of excitation of the  $^{57}\text{Fe}$  hyperfine line. Since most of the excitation is through the 2p levels, and the excitation energy of these levels is

much less than the temperature at which Fe XXIV is most abundant, this correction for resonances is small.

The resulting values of the effective collision strength as a function of temperature are shown in Figure 5. When the electron collision are dominated by direct excitation and/or allowed collisional excitation followed by direct decay to the ground hyperfine sublevels, the excitation and de-excitation rates obey detailed balance, and the same effective collision strength applies to both excitation and de-excitation. This is the case for the  $^{57}\text{Fe}$  hyperfine line.

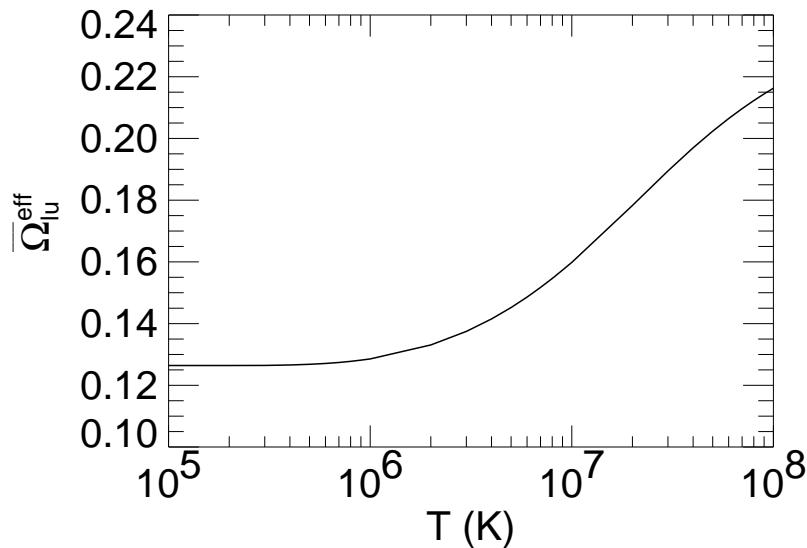


Fig. 5.— Thermally-averaged effective collision strength for excitation and de-excitation of the  $^{57}\text{Fe}$  hyperfine line versus temperature.

### 3.6. *Optical Pumping*

The same indirect electron collisional excitation processes which dominate the collisional excitation of the  $^{57}\text{Fe}$  hyperfine line also produce EUV and X-ray photons. The  $2s - 2p$  excitations produce EUV lines at  $192 \text{ \AA}$  and  $255 \text{ \AA}$ , while the  $2s - 3p$  excitations make an X-ray doublet at  $10.6 \text{ \AA}$ . Photons in these lines, due to the collisional excitation of  $\text{Fe}^{+23}$  or due to some unrelated continuum process, can be absorbed by this ion, and this radiative excitation will normally be followed by a radiative decay. This resonant scattering process can also affect the excitation of the ground hyperfine sublevels through the branching ratios of the radiative cascades to the sublevels (Sunyaev & Churazov 1984). We refer to this



process as “optical pumping.”

Let  $n_l R_{lu}(nSLJ)$  be the rate of excitation per unit volume of ions in the lower ground hyperfine sublevel to the upper ground hyperfine sublevel through the resonant scattering of a line whose upper level is denoted by the quantum numbers  $(nSLJ)$ . Let  $\bar{J}(nSLJ)$  be the line profile averaged mean intensity of this EUV or X-ray line, which is defined by

$$\bar{J}(nSLJ) \equiv \int J_\nu(nSLJ) \phi(\nu) d\nu. \quad (17)$$

Here,  $\phi(\nu)$  is the line profile function, which is normalized so that its integral over all frequencies is unity. The mean intensity of the line,  $J_\nu(nSLJ)$ , is averaged over all directions. Then, it is straightforward to show that

$$R_{lu}(nSLJ) = \left[ \frac{c^2 \bar{J}(nSLJ)}{2h\nu^3} \right] \sum_F \frac{2F+1}{2F_l+1} \frac{A(F, F_l)A(F, F_u)}{\sum_{F'} A(F, F')}, \quad (18)$$

where  $\nu$  is the central frequency of the line,  $F$  denotes a hyperfine sublevel of the upper level  $nSLJ$ , and  $A(F, F')$  is the radiative decay rate of the upper hyperfine sublevel to one of the ground hyperfine sublevels,  $F' = F_l, F_u$ . If one ignores the small difference in  $\bar{J}(nSLJ)$  for the hyperfine components of the line, the symmetrical occurrence of  $F_u$  and  $F_l$  in the radiative decay rate in equation (18) would imply the detailed balance relation  $g_l R_{lu} = g_u R_{ul}$ . When one includes the finite hyperfine splitting of the ground level and treats the line profile in detail including recoil, the relationship for an optically thick line becomes (Field 1959)

$$g_l R_{lu} = g_u R_{ul} \exp\left(\frac{-\Delta E_{lu}}{kT}\right). \quad (19)$$

Equation (18) can be evaluated easily using equations (5) and (6). For any of the important resonance lines in Fe XXIV (2s—2p 192 Å and 255 Å, and 2s—3p 10.6 Å), one finds that

$$R_{lu}(nSLJ) = \frac{2}{3} \left[ \frac{c^2 \bar{J}(nSLJ)}{2h\nu^3} \right] A(nSLJ, 2s \ ^2S_{1/2}), \quad (20)$$

where  $A(nSLJ, 2s \ ^2S_{1/2})$  is the radiative decay rate to the ground level ignoring the hyperfine structure. Thus, the rate of optical pumping is simply related to the total rate of absorption of the line photons.

If the photons being resonantly scattered originated through collisional excitation of  $\text{Fe}^{+23}$ , optical pumping can be thought of as increasing the effective rate of indirect collisional excitation. Crudely, the average rate of collisional excitation will be increased by a factor which is of the order of the optical depth of the line. Under some circumstances, the lines could be moderately optically thick (optical depths  $\lesssim 10^2$ ), and optical pumping might be

quite important (Sunyaev & Churazov 1984). Because of radiative transfer, this is a nonlocal process, which depends on the global structure of the system and on the velocity fields. As a result, we don't discuss optical pumping any further in this paper. In Paper II, we include optical pumping in determining the excitation of the  $^{57}\text{Fe}$  hyperfine line in clusters of galaxies and cooling flows.

#### 4. LEVEL POPULATIONS AND RADIATIVE EXCITATION

Because the  $^{57}\text{Fe}$  hyperfine line wavelength is near the peak of the Cosmic Microwave Background Radiation (CMBR), it is important to include the stimulated radiative processes as well as spontaneous decay. The rates of stimulated emission and absorption are given by  $B_{ul}\bar{J}$  and  $B_{lu}\bar{J}$ , respectively. The Einstein coefficients  $B_{ul}$  and  $B_{lu}$  are related to the rate for spontaneous decay,  $A_{ul}$ , by the Einstein relations,

$$B_{ul} = \frac{g_l B_{lu}}{g_u} = \frac{c^2}{2h\nu_o^3} A_{ul}, \quad (21)$$

where  $\nu_o = \Delta E_{lu}/h$  is the line-center frequency of the line. The quantity  $\bar{J}$  is the line profile averaged mean intensity of the radiation at the  $^{57}\text{Fe}$  hyperfine line (e.g., eq. [17]).

The CMBR is a blackbody at a temperature of  $T_R = 2.73$  K. Since the hyperfine line wavelength is near the peak of the CMBR, one has to use the Planck function without any approximations. However, the line profile of the hyperfine line is expected to be fairly narrow, and the line profile averaged mean intensity should be given accurately by the blackbody intensity at the line center,  $\bar{J} = B_{\nu_o}(T_R)$ , where  $B_{\nu}(T)$  is the blackbody spectrum.

The time scales for excitation and de-excitation of the 2s hyperfine levels are much shorter than the ages or any other interesting time scales in most astrophysical systems of interest. Thus, we assume that the hyperfine levels are in statistical equilibrium,

$$n_u (A_{ul} + B_{ul}\bar{J} + n_e q_{ul}) = n_l (B_{lu}\bar{J} + n_e q_{lu}). \quad (22)$$

Here,  $n_u$  and  $n_l$  are the number density of ions in the upper and lower hyperfine sublevels, respectively. The total rate coefficient for collisional excitation,  $q_{lu}$ , is determined by replacing the collision strength  $\bar{\Omega}_{lu}$  with the effective collision strength  $\bar{\Omega}_{lu}^{\text{eff}}$  in equation (3). The effective collision strength is given in equation (16) and Figure 5.

The collisional excitation and de-excitation rates are related by detailed balance,

$$q_{lu} = \frac{g_u}{g_l} q_{ul} \exp\left(-\frac{\Delta E_{lu}}{kT}\right). \quad (23)$$

Similarly, the Einstein relations (eq. 21) can be used to substitute for  $B_{lu}$  and  $B_{ul}$  in terms of  $A_{ul}$ . With these simplifications, equation (22) can be solved for the ratio of the occupancy of the upper and lower hyperfine sublevels:

$$\frac{n_u}{n_l} = \frac{g_u}{g_l} \exp\left(-\frac{\Delta E_{lu}}{kT}\right) \left\{ \frac{1 + \left(\frac{A_{ul}}{n_e q_{ul}}\right) \left(\frac{\bar{J}c^2}{2h\nu_o^3}\right) \exp(+\Delta E_{lu}/kT)}{1 + \left(\frac{A_{ul}}{n_e q_{ul}}\right) \left[1 + \left(\frac{\bar{J}c^2}{2h\nu_o^3}\right)\right]} \right\}. \quad (24)$$

The quantity  $[(\bar{J}c^2)/(2h\nu_o^3)]$  is the photon occupation number of the radiation field at the frequency of the line.

The above expression implies that when the electron density is very high, the ratio of level populations approaches LTE at the electron kinetic temperature  $T$ . Given the very small excitation energy  $\Delta E_{lu}$ , this implies that the ratio of level populations approaches that of the statistical weights,  $(n_u/n_l) = 3$ , at high densities. It is useful to define a critical electron density as

$$n_{e,cr} \equiv \frac{A_{ul}}{q_{ul}} \left[1 + \left(\frac{\bar{J}c^2}{2h\nu_o^3}\right)\right] \approx 17 \left(\frac{T}{1.8 \times 10^7 \text{ K}}\right)^{1/2} \text{ cm}^{-3}, \quad (25)$$

such that the rates of radiative and collisional de-excitation are equal at this density. The numerical value in equation (25) assumes that the radiation field is the CMBR at a temperature of 2.73 K, and the temperature  $1.8 \times 10^7$  K is the value at which the ionization fraction of  $\text{Fe}^{+23}$  is maximum in collisional ionization equilibrium (see Figure 6). The electron density must be at least this high for the level populations to approach LTE at the electron kinetic temperature. In most astrophysical situations where the  $^{57}\text{Fe}$  line would be produced, the density is considerably less than  $n_{e,cr}$ .

On the other hand, all astrophysical plasmas are immersed in the CMBR. In the limit of very low densities, the level populations due to the CMBR are given by

$$\frac{n_u}{n_l} = \frac{g_u}{g_l} \exp\left(-\frac{\Delta E_{lu}}{kT_R}\right) \approx 0.538. \quad (26)$$

for the temperature of the CMBR in the nearby (i.e., low redshift) universe. Thus, the upper hyperfine level is significantly populated even when there is no collisional excitation.

Because we are most interested in the excitation of the hyperfine line under low density conditions, it is useful to define a small parameter  $\epsilon$  as

$$\epsilon \equiv \frac{n_e}{n_{e,cr}}. \quad (27)$$

Then, in the low density limit, the population is given to first order in  $\epsilon$  as

$$\frac{n_u}{n_l} \approx \frac{g_u}{g_l} \exp\left(-\frac{h\nu_o}{kT_R}\right) \left\{1 + \epsilon \left[\exp\left(\frac{h\nu_o}{kT_R}\right) - 1\right]\right\}. \quad (28)$$

## 5. RADIATIVE TRANSFER

The emissivity,  $j_\nu$ , and the absorption coefficient,  $\kappa_\nu$ , of the hyperfine line are given by

$$j_\nu = \frac{h\nu}{4\pi} A_{ul} n_u \phi(\nu), \quad (29)$$

and

$$\kappa_\nu = \frac{A_{ul} c^2 \phi(\nu)}{8\pi\nu^2} g_u \frac{n_l}{g_l} \left( 1 - \frac{n_u g_l}{g_u n_l} \right). \quad (30)$$

The source function for the line,  $S$ , is

$$S \equiv \frac{j_\nu}{\kappa_\nu} = \frac{2h\nu_o^3}{c^2} \frac{n_u g_l}{g_u n_l} \left( 1 - \frac{n_u g_l}{g_u n_l} \right)^{-1}. \quad (31)$$

In the low density limit (eq. 28), the source function is approximately

$$S \approx B_{\nu_o}(T_R) \left\{ 1 + \epsilon \left[ \exp\left(\frac{h\nu_o}{kT_R}\right) - 1 \right] \right\}, \quad (32)$$

Typically, the intensity of the line will be much less than that of the CMBR, and we can take  $T_R = 2.73$  K.

For the moment, we will assume that an emission region producing the hyperfine line is homogeneous. Then, the solution of the radiative transfer equation for the intensity,  $I_\nu$ , along any given line-of-sight through the region is

$$I_\nu = I_\nu^o \exp(-\tau_\nu) + S [1 - \exp(-\tau_\nu)], \quad (33)$$

where  $I_\nu^o$  is the incident intensity on the far side of the region. The optical depth is  $\tau_\nu \equiv \int \kappa_\nu ds$ , where  $s$  is the path length along the line-of-sight.

The directly observable quantity is not the brightness of the line, but the difference between the line and the background radiation  $I_\nu^o$ . This difference is

$$\Delta I_\nu \equiv (I_\nu - I_\nu^o) = (S - I_\nu^o) [1 - \exp(-\tau_\nu)]. \quad (34)$$

In most astrophysical environments, the line will be very optically thin,  $\tau_\nu \ll 1$ . Moreover, the background radiation will most often be the CMBR, and the line will be much weaker than the CMBR. Thus, we can take  $I_\nu^o = B_\nu(T_R)$ . All of the  $^{57}\text{Fe}^{+23}$  ions are assumed to be in one of the two hyperfine levels, so that  $n(^{57}\text{Fe}^{+23}) = (n_u + n_l)$ . Then, if the low density expression for the source function (eq. 32) is substituted into equation (34) and the exponential of the optical depth is expanded, the resulting net intensity is

$$\Delta I_\nu = \frac{h\nu_o}{4\pi} D(T_R) \int n_e n(^{57}\text{Fe}^{+23}) q_{lu} \phi(\nu) ds. \quad (35)$$

The correction factor for radiative excitation of the hyperfine structure  $D(T_R)$  is

$$D(T_R) \equiv \frac{1 - \exp(-h\nu_o/kT_R)}{1 + \frac{g_u}{g_l} \exp(-h\nu_o/kT_R)} = 0.533 \text{ for } T_R = 2.73 \text{ K.} \quad (36)$$

Thus, the line intensity is reduced by about a factor of two below that expected if there were no radiative excitation of the levels and all of the electrons were in the lower hyperfine sublevel  $l$ . Note that this factor depends somewhat on the redshift  $z$  of the emitter, since  $T_R = 2.73(1 + z)$ .

For completeness, we note that the hyperfine line intensity in the astrophysically less interesting high density limit ( $n_e \gg n_{e,cr}$ ) is given by

$$\Delta I_\nu = \frac{h\nu_o}{4\pi} \frac{g_u}{g_u + g_l} A_{ul} \int n(^{57}\text{Fe}^{+23}) \phi(\nu) ds, \quad (37)$$

which is equivalent to the expression for the intensity of the 21 cm H I line. The fraction of the ions in the upper hyperfine sublevel (the second factor in eq. [37]) is 3/4, as in hydrogen.

## 6. RESULTING LINE INTENSITIES

We adopted an solar iron abundance of  $\text{Fe}/\text{H} = 4.68 \times 10^{-5}$  by number (Anders & Grevesse 1989). The solar system value of the fraction of iron which is  $^{57}\text{Fe}$  was taken to be 2.3% (Völkening & Papanastassiou 1989). For consistency with the rates of ionization and emission used in many analyses of the X-ray emission of hot plasmas, we used the same atomic physics rates as used in the MEKAL X-ray emission code (e.g., Kaastra et al. 1996), as presented in version 10 of the XSPEC spectral analysis package. The MEKAL program includes some recent improvements in the treatment of the Fe L X-ray lines, including the lines from Fe XXIV (e.g., Liedahl et al. 1995). The ionization and recombination rates in the MEKAL code are basically those from Arnaud & Rothenflug (1985). The ionization fraction of  $\text{Fe}^{+23}$  as a function of temperature is shown in Figure 6.

The luminosity of the hyperfine line in the low density limit can be written as

$$L_{hf} = \Lambda_{hf}(T) \int n_p n_e dV, \quad (38)$$

where the gas is assumed to be isothermal and in collisional ionization equilibrium. The integral is the standard integrated emission measure or emission integral of the plasma, where  $n_p$  is the proton number density and  $V$  is the volume of the gas. The emissivity coefficient  $\Lambda_{hf}(T)$  is shown in Figure 7 for solar abundances; it is proportional to the abundance of  $^{57}\text{Fe}$ . In calculating the values in Figure 7, we included ionization and recombination in the

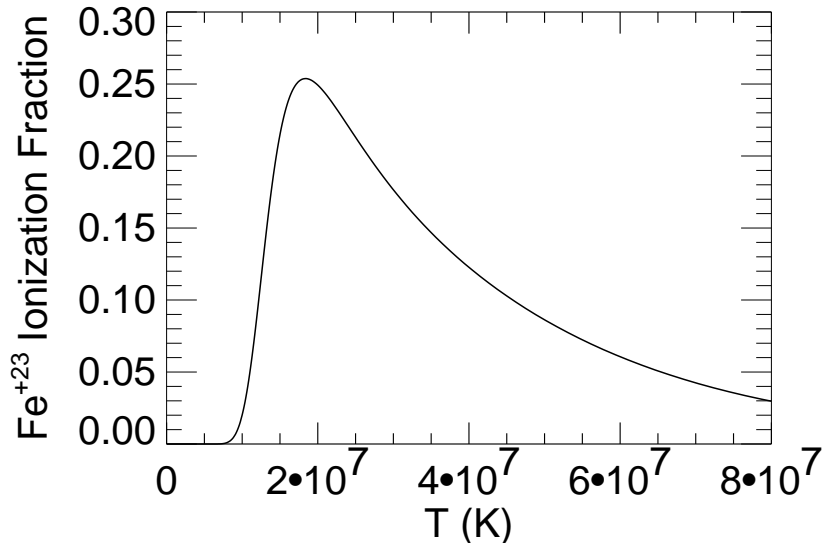


Fig. 6.— The ionization fraction of  $\text{Fe}^{+23}$  as a function of temperature. The ionization fraction peaks at a temperature of about  $1.8 \times 10^7$  K.

line excitation. By comparing Figures 6 and 7, it is clear that the temperature dependence of the emissivity coefficient is mainly due to the variation of the ionization fraction of  $\text{Fe}^{+23}$  with temperature. The emissivity coefficient peaks around  $1.8 \times 10^7$  K.

In the paper which originally suggested that the  $^{57}\text{Fe}$  line might be of astrophysical interest, Sunyaev & Churazov (1984) estimated the excitation rate of the  $^{57}\text{Fe}$  line along with many other hyperfine lines. For fixed abundances and ionization fractions, their estimate of the line excitation rate is about a factor of three higher than our values. They estimated that one-half of all excitations of the 2p levels lead to excitations of the upper hyperfine level. The actual ratio is slightly lower (4/9 at high energies; see Tables 1 and 2). The primary difference would seem to be that their values for the 2s–2p excitation rates are about a factor of three higher than ours. There is some ambiguity in their paper between the definitions of excitation and de-excitation rates, and their expression for the excitation rate may have an extra factor of  $(g_u/g_l)$ . This could account for the difference in excitation rates. When it comes to determining the emissivity of the gas at a given temperature, their values exceed ours by a larger factor, because of the assumption of a higher peak ionization fraction for  $\text{Fe}^{+23}$ . On the other hand, their adopted solar abundance for  $^{57}\text{Fe}$  is slightly lower than ours. In any case, it is clear that the intent of the Sunyaev & Churazov paper was only to give crude estimates of the intensities of a large number of hyperfine lines to support the suggestion that they might be observable.

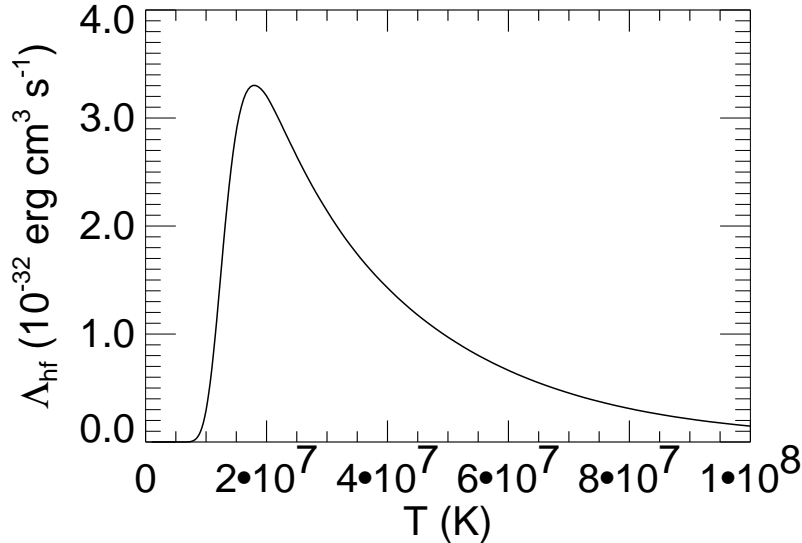


Fig. 7.— The emissivity coefficient  $\Lambda_{hf}(T)$  of the  $^{57}\text{Fe}^{+23}$  hyperfine line as a function of temperature, assuming solar abundances and collisional ionization equilibrium. The temperature dependence is mainly due to the ionization fraction of  $\text{Fe}^{+23}$  and hence peaks at a temperature of  $1.8 \times 10^7$  K.

We also calculated the emission of the hyperfine line in a plasma cooling isobarically due to its own radiation, in the low density limit. The luminosity of the hyperfine line in gas cooling from a temperature  $T$  is given by (White & Sarazin 1987)

$$L_{hf} = \dot{M} \left[ \frac{5}{2} \frac{k}{\mu m_H} \int_0^T \frac{\Lambda_{hf}(T')}{\Lambda(T')} dT' \right] = \Gamma_{hf}(T) \dot{M}, \quad (39)$$

where  $\Lambda_{hf}(T)$  is the emissivity coefficient of the hyperfine line,  $\Lambda(T)$  is the coefficient for the total emissivity of the gas (also sometimes called the cooling function),  $\mu$  is the mass per particle in the gas in units of the mass of the hydrogen atom  $m_H$ , and  $\dot{M}$  is the rate at which gas is cooling (in  $\text{g s}^{-1}$ ). The function  $\Gamma_{hf}(T)$  is defined by the quantity in brackets in equation (39), and is given in Figure 8.  $\Gamma_{hf}(T)$  gives the emission per unit mass of cooling gas, as a function of the initial temperature of the gas. Again, we used the cooling function derived from the MEKAL code as presented in XSPEC (version 10). Solar abundances are used in computing the luminosity. The value of  $\Gamma_{hf}$  rises rapidly with temperature through the value at which the  $\text{Fe}^{+23}$  ion is most abundant,  $1.8 \times 10^7$  K. At temperatures greater than about  $7 \times 10^7$  K, the value of  $\Gamma_{hf}$  flattens out, since all gas which starts at higher temperature passes completely through the temperature range where the line is emitted strongly.

For the purpose of determining the fraction of iron which is  $^{57}\text{Fe}$ , it is more useful to compare the strength of the hyperfine line to other iron lines. In particular, if the comparison

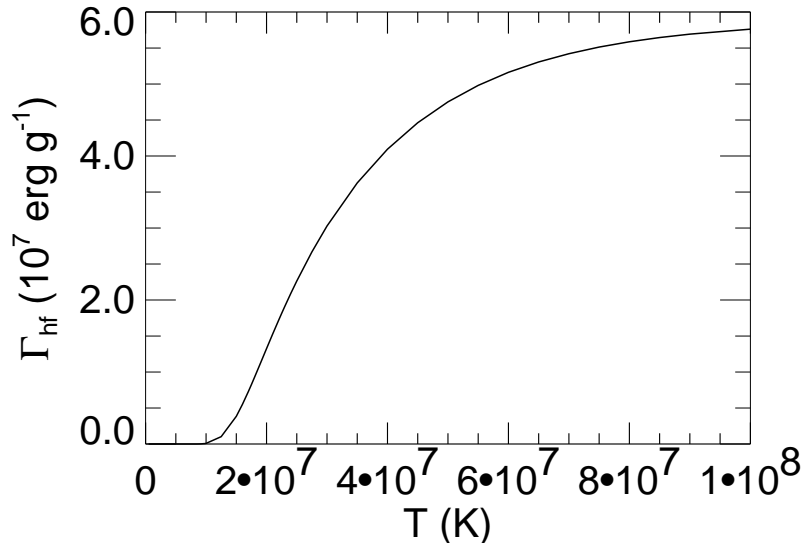


Fig. 8.— The emission of the  $^{57}\text{Fe}^{+23}$  hyperfine line from a gas cooling isobarically subject to its own radiation. The function  $\Gamma_{hf}(T)$  gives the energy radiated per unit mass of cooling gas, as a function of the initial temperature of the gas (eq. 39). Solar abundances and collisional ionization equilibrium are assumed.

is made to lines produced by the same ion  $\text{Fe}^{+23}$ , then the derived fractional abundance of  $^{57}\text{Fe}$  is nearly independent of the ionization structure in the gas. On the other hand, the absolute flux of the hyperfine line is very strongly affected by the ionization structure, as is seen in Fig. 7.

In principle, the best lines for this purpose are the  $\text{Fe}^{+23}$   $2s - 2p$  lines, which are  $2s\ ^2\text{S}_{1/2} - 2p\ ^2\text{P}_{3/2}$  192.02 Å and  $2s\ ^2\text{S}_{1/2} - 2p\ ^2\text{P}_{1/2}$  255.10 Å. These lines are excited by same collisional excitations which we have found to be the main excitation source for the  $\text{Fe}^{+23}$  hyperfine line. As a result, the ratio of the luminosity of the hyperfine line to the luminosity of either of these two extreme ultraviolet (EUV) lines is nearly independent of the temperature or ionization state of the gas. To the extent that the excitation of the hyperfine line is dominated by  $2s-2p$  collisional excitations, the line ratios depend mainly on the wavelengths of the lines, the fractional abundance of  $\text{Fe}^{+23}$ , the radiative correction factor  $D(T_R)$  (eq. 36), and the branching ratios (Table 2). For example, in the limit where  $2s-2p$  excitations dominate the hyperfine line and the temperature is much greater than the excitation energy of these transitions, the luminosity ratio to the  $2s\ ^2\text{S}_{1/2} - 2p\ ^2\text{P}_{3/2}$  192.02 Å line is

$$\frac{L(hf)}{L(192\text{ \AA})} \approx \frac{2}{3} D(T_R) \left( \frac{192\text{ \AA}}{3.071\text{ mm}} \right) \left[ \frac{n(^{57}\text{Fe})}{n(\text{Fe})} \right] \approx 2.2 \times 10^{-6} \left[ \frac{n(^{57}\text{Fe})}{n(\text{Fe})} \right]. \quad (40)$$



The term in brackets is the relative abundance of  $^{57}\text{Fe}$ . The equivalent result for the other EUV line ( $2s\ ^2S_{1/2} - 2p\ ^2P_{1/2}$  255.10 Å) is

$$\frac{L(hf)}{L(255\ \text{Å})} \approx \frac{4}{3} D(T_R) \left( \frac{255\ \text{Å}}{3.071\ \text{mm}} \right) \left[ \frac{n(^{57}\text{Fe})}{n(\text{Fe})} \right] \approx 5.9 \times 10^{-6} \left[ \frac{n(^{57}\text{Fe})}{n(\text{Fe})} \right]. \quad (41)$$

In Figure 9, the  $L(hf)/L(192\ \text{Å})$  line ratio is given from a more detailed calculation including all excitation processes for both lines, and assuming the solar isotope fraction of  $^{57}\text{Fe}$  of 2.3%. The 192 Å line was calculated using the MEKAL code. Other excitation processes produce a slight temperature variation and increase the line ratio by about 20% above the analytical estimate at about 120 Ryd. As the temperature increases above  $2 \times 10^7$  K, the ionization fraction of  $\text{Fe}^{+23}$  decreases (Figure 6), and recombination from  $\text{Fe}^{+24}$  to  $\text{Fe}^{+23}$  becomes an important excitation process for both the hyperfine line and the 192 Å line. This causes the increase in the line ratio at high temperatures as seen in Figure 9.

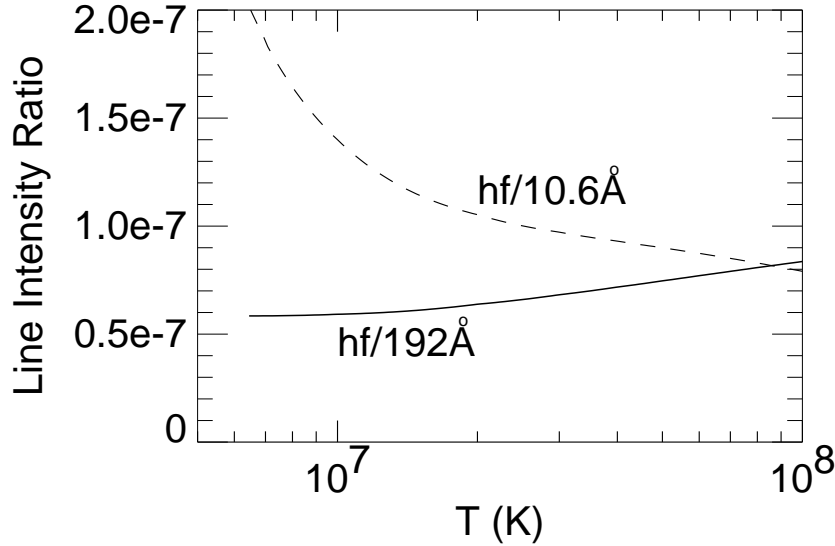


Fig. 9.— The ratios of the luminosity of the  $^{57}\text{Fe}^{+23}$  hyperfine line to the strongest EUV and X-ray lines from  $\text{Fe}^{+23}$ . The solid curve is the ratio to the EUV line  $2s\ ^2S_{1/2} - 2p\ ^2P_{3/2}$  192.02 Å line, while the dashed curve is the ratio to the  $2s\ ^2S_{1/2} - 3p\ ^2P_{1/2,3/2}$  10.663, 10.619 Å doublet.

One negative feature of the 2s—2p EUV lines is that they are in a part of the spectrum which is difficult to observe, partly because of Galactic absorption. Moreover, their fluxes might be uncertain even if detected because of the correction for absorption. The 2s—3p X-ray lines from  $\text{Fe}^{+23}$  are easier to observe, and less subject to absorption. An alternative standard of comparison might be the allowed doublet of 2s—3p lines,  $2s\ ^2S_{1/2} - 3p\ ^2P_{3/2}$

10.619 Å and  $2s\ 2S_{1/2} - 3p\ 2P_{1/2}$  10.663 Å. Because this doublet is difficult to resolve, we consider the luminosity  $L(10.6\ \text{Å})$  of the sum of the two lines. The ratio of the hyperfine line to this doublet is also shown in Figure 9. The 10.6 Å line was calculated using the MEKAL code. Due to the higher excitation energy of this doublet and the difference in the temperature dependence of the collision strengths exciting the hyperfine line and the  $2s-3p$  X-ray doublet, this line ratio is much more temperature dependent.

The observability of this line is crucially dependent on its wavelength. We use a wavelength value of 3.071 mm from the paper by Shabaeva & Shabaev (1992). The uncertainty in this number is about 0.15% (Shabaev, Shabaeva & Tupitsyn 1995), which translates into a velocity uncertainty of about  $450\ \text{km s}^{-1}$ . This is larger than the bandwidth of many radio spectrometers in this wavelength region. On the other hand, the widths of the  $^{57}\text{Fe}$  lines expected in astrophysical environments may well be even broader (e.g., Paper II). Hence undertaking observations of this line will be difficult unless a spectrometer with a large bandwidth is used. We will discuss the detectability of this line further in Paper II.

## 7. SUMMARY

Sunyaev & Churazov (1984) first showed that the 3.071 mm hyperfine line from Li-like  $^{57}\text{Fe}$  might be observable in astrophysical plasmas. We have assessed the various atomic processes that can contribute to the excitation of this line. We calculated the rate of direct electron collisional excitation of the upper hyperfine level, and found it to be small. The rate of proton collisional excitation was shown to be negligible. We calculate the rate of excitation of the line by electron collisional excitation of more highly excited states, followed by radiative cascade. We derive the branching ratios for allowed radiative decays to different hyperfine sublevels, and the resulting cascade matrix. We also derive branching ratios for the electron collisional excitation of hyperfine sublevels for direct and exchange interactions.

As originally suggested by Sunyaev & Churazov (1984), the dominant process in the excitation of the 3.071 mm hyperfine line is electron collisional excitation of the  $2p$  levels, followed by cascade. We calculate the excitation rates for this process, and show that they are dominated by radiatively allowed transitions, for which the collision strengths can be derived easily from existing calculations of the collision strengths and the branching ratios. We derive an effective collision strength for exciting the hyperfine line which includes the direct collisional excitation, the excitation of the  $2p$  levels and higher levels, cascades, and a correction for resonances.

At the wavelength of the 3.071 mm hyperfine line, induced radiative transitions due

to the Cosmic Microwave Background Radiation (and possibly, other microwave radiation sources) are important. We calculate the effect of the CMBR on the level populations and line excitation. We determine the net intensity of the line above the background radiation. The plasmas that radiate the hyperfine line will most likely have electron densities that are much lower than the electron densities at which radiative decays and collisional excitation are balanced. Thus, we derive expressions for the net line intensity in this low density limit.

We determine the intensity of the hyperfine line from an isothermal, coronal plasma in collisional ionization equilibrium with solar abundances. Because collisional excitation of the line varies slowly with is mainly due to the variation in the ionization fraction of  $\text{Fe}^{+23}$ . For a given emission measure, the line intensity is maximum at a temperature of about  $1.8 \times 10^7$  K. Our emission rates are somewhat smaller than the estimates given by Sunyaev & Churazov (1984). We have also derived the hyperfine line luminosity emitted by a coronal plasma cooling isobarically due to its own radiation.

Because of the strong dependence of the hyperfine line emissivity on the ionization state of the gas, the isotopic abundance of  $^{57}\text{Fe}$  relative to the total iron abundance is best determined by comparing the hyperfine line to other lines emitted by the same ion,  $\text{Fe}^{+23}$ . We suggest that ratios to the 2s—2p EUV lines at 192 Å and 255 Å or the 2s—3p X-ray lines at 10.6 Å be used to derive isotopic abundances. We derive these line ratios as a function of temperature.

In Paper II, we will apply these results to predict the properties of the 3.071 mm  $^{57}\text{Fe}^{+23}$  hyperfine line from cooling flow and non-cooling flow clusters of galaxies.

**Acknowledgements** C. L. S. was supported in part by NASA Astrophysical Theory Program grant 5-3057. We thank Bob Brown, Eugene Churazov, Dave Frayer, and Rashid Sunyaev for useful comments. We thank Doug Sampson for sending up his results in advance of publication.

## REFERENCES

- Alder, K., Bohr, A., Huus, T., Mottleson, B., & Winther, A. 1956, *Rev. Mod. Phys.*, 28, 432  
 Anders, E., & Grevesse, N. 1989, *Geochim. Cosmochim. Acta*, 53, 197  
 Arnaud, M., & Rothenflug, M. 1985, *A&AS*, 60, 425  
 Bahcall, J. N., & Wolf, R. A. 1968, *ApJ*, 152, 701  
 Balser, D. S., Bania, T. M., Rood, R. T., & Wilson, T. L. 1997, *ApJ*, 483, 320  
 Bely, O., & Faucher, P. 1970, *A&A*, 6, 88  
 Clark, R. E. H., Magee, Jr., N. H., Mann, J. B., & Merts, A. L. 1982, *ApJ*, 254, 412  
 D’Cruz, N. L., & Sarazin, C. L. 1998, in preparation (Paper II)  
 Dickey, J. M., & Lockman, F. J. 1990, *ARA&A*, 28, 215  
 Eissner & Seaton, M. J. 1972, *J. Phys. B*, 5, 2187

- Field, G. B. 1959, *ApJ*, 129, 551
- Gallagher, J. W., & Pradhan, A. K. 1985, An Evaluated Compilation of Data for Electron-Impact Excitation of Atomic Ions, JILA Information Center Rept. No. 30 (Boulder: University of Colorado), 172
- Hayes, M. A. 1979, *MNRAS*, 189, 49p
- Kaastra, J. S., Mewe, R., Liedahl, D. A., Singh, K. P., White, N. E., & Drake, S. A. 1996, *A&A*, 314, 547
- Kastner, S. O. 1977, *A&A*, 54, 255
- Kastner, S. O., & Bhatia, A. K. 1979, *A&A*, 71, 211
- Liedahl, D. A., Osterheld, A. L., & Goldstein, W. H. 1995, *ApJ*, 438, L115
- Lubowich, D. A., Anantharamiah, K. R., & Pasachoff, J. M. 1989 *ApJ*, 345, 770
- Mann, J. B. 1983, *At. Data Nucl. Data Tables*, 29, 407
- Mason, H. E. 1975, *MNRAS*, 170, 651
- Petrini, D. 1970, *A&A*, 9, 392
- Rood, R. T., Bania, T. M., Wilson, T. L., & Balsler, D. S. 1995, in *ESO/EIPC Workshop on the Light Elements*, ed. P. Crane (Heidelberg: Springer), 201
- Sampson, D. H., & Zhang, H. L. 1997, *J. Phys. B: At. Mol. Opt. Phys.*, 30, 28
- Saraph, H. E. 1978, *Comp. Phys. Comm.*, 15, 247
- Seaton, M. J. 1964, *MNRAS*, 127, 191
- Seaton, M. J. 1966, *Proc. Physical Soc.*, 88, 801
- Shabaeva, M. B., & Shabaev, V. M. 1992, *Phys. Lett. A*, 165, 72
- Shabaev, V. M., Shabaeva, M. B. & Tupitsyn, I. I. 1995, *Phys. Rev. A*, 52, 3686
- Sunyaev, R. A., & Churazov, E. M. 1984, *Soviet Ast. Lett.*, 10, 201
- Van Regemorter, H. 1962, *ApJ*, 136, 906
- Völkening, J., & Papanastassiou, D. A. 1989, *ApJ*, 347, L43
- White, R. E., & Sarazin, C. L. 1987, *ApJ*, 318, 621

# EXCITATION OF THE 3.071 mm HYPERFINE LINE IN Li-LIKE $^{57}\text{Fe}$ IN ASTROPHYSICAL PLASMAS

NOELLA L. D'CRUZ AND CRAIG L. SARAZIN  
Department of Astronomy, University of Virginia,  
P.O. Box 3818, Charlottesville, VA 22903-0818;  
nld2n@virginia.edu, cls7i@virginia.edu

and

JACQUES DUBAU  
Observatoire de Paris, F 92195 Meudon Principal Cedex, France;  
dubau@delacroix.obspm.fr

*Accepted for publication by the Astrophysical Journal, 27 Jan 1998*

## ABSTRACT

As noted first by Sunyaev & Churazov (1984), the 3.071 mm hyperfine line from  $^{57}\text{Fe}^{+23}$  might be observable in astrophysical plasmas. We assess the atomic processes which might contribute to the excitation of this line. The distorted wave approximation was used to compute the direct electron collision strength between the two hyperfine sublevels of the ground configuration; it was found to be small. Proton collisional excitation was calculated and found to be negligible. We determine the rate of line excitation by electron collisional excitation of more highly excited levels, followed by radiative cascades. The branching ratios for hyperfine sublevels for allowed radiative decays and electron collisional excitation or de-excitation are derived. We show that the dominant line excitation process is electron collisional excitation of the 2p levels followed by radiative decay, as first suggested by Sunyaev & Churazov (1984). We calculate an effective collision strength for excitation of the hyperfine line, including all of these effects and correcting for resonances. Because the hyperfine line is near the peak in the Cosmic Microwave Background Radiation spectrum, induced radiative processes are also very important. The effect of background radiation on the level populations and line excitation is determined.

We determine the intensity of the hyperfine line from an isothermal, coronal plasma in collisional ionization equilibrium. Because of the variation in the ionization fraction of  $\text{Fe}^{+23}$ , the emissivity peaks at a temperature of about  $1.8 \times 10^7$  K. We have also derived the hyperfine line luminosity emitted by a coronal plasma

cooling isobarically due to its own radiation. Comparisons of the hyperfine line to other lines emitted by the same ion,  $\text{Fe}^{+23}$ , are shown to be useful for deriving the isotopic fraction of  $^{57}\text{Fe}$ . We calculate the ratios of the hyperfine line to the 2s—2p EUV lines at 192 Å and 255 Å, and the 2s–3p X-ray doublet at 10.6 Å.

*Subject headings:* atomic data — atomic processes — hyperfine structure — line formation — radiative transfer — radio lines: general

## 1. INTRODUCTION

Astrophysically, the most important and well studied atom exhibiting hyperfine structure is the neutral hydrogen atom. Its hyperfine transition at 21 cm has been observed for many years both in emission and absorption in the gas in our Galaxy and other galaxies, and has provided information on the velocity structure of these systems (see Dickey & Lockman 1990 for a review). Besides this line, hyperfine emission from  $^3\text{He}$  has also been observed in our Galaxy in planetary nebulae (Balsler et al. 1997) and H II regions (Rood et al. 1995). There have also been a number of searches for the 92 cm hyperfine line in deuterium (e.g., Lubowich, Anantharamiah, & Pasachoff 1989). In this paper, we are concerned with another atomic hyperfine transition which could possibly be of astrophysical interest — the 3.071 mm line (Shabaeva & Shabaev 1992) in Li-like  $^{57}\text{Fe}$ . As originally suggested by Sunyaev & Churazov (1984), it is potentially observable in a variety of astrophysical systems containing very diffuse, hot plasma ( $T \sim 10^7$  K), including clusters of galaxies, elliptical galaxies, hot interstellar gas in our own Galaxy, and supernova remnants. In a related paper, we calculate the line intensities expected from cooling flow and non-cooling flow clusters of galaxies (D’Cruz & Sarazin 1997; hereafter Paper II).

In the hot plasmas which would emit the  $^{57}\text{Fe}$  hyperfine line, the dominant radiation is X-ray line and continuum emission. However, observations of the  $^{57}\text{Fe}$  hyperfine line might have several advantages compared to X-ray line observations of the same plasma. First, the atmospheric absorption at 3.071 mm is low enough to allow ground based observations with large radio telescopes. Second, the spectral resolution of radio detectors vastly exceeds that of all existing or planned astrophysical X-ray spectrometers. Thus, observations of the 3.071 mm line could be used to determine the velocity field (bulk motions, turbulence, and thermal velocities) in the hot gas in clusters of galaxies and supernova remnants. Third, the detection of this  $^{57}\text{Fe}$  hyperfine line would allow the abundance of this isotope to be determined relative to the more common  $^{56}\text{Fe}$  isotope. Since these two isotopes are produced by different nuclear processes, this would provide a powerful constraint of nucleosynthesis in supernova remnants and on the chemical history of the intracluster gas. In this regard, the most direct measure of the isotope ratio comes from the ratio of the radio line from  $^{57}\text{Fe}$  to the EUV and X-ray lines from the same ion, Fe XXIV.

The 3.071 mm hyperfine line arises from the ground level ( $1s^2 2s \ ^2S_{1/2}$ ) of  $^{57}\text{Fe}$  XXIV. The nuclear spin of the  $^{57}\text{Fe}$  isotope is  $I = 1/2$ , so the total angular momentum is  $F = 0$  or 1. We denote the lower hyperfine sublevel ( $F = 0$ ) with the subscript  $l$ , and the upper hyperfine sublevel ( $F = 1$ ) with the subscript  $u$ . The statistical weights of the hyperfine sublevels are  $g_l = 1$  and  $g_u = 3$ . The rate of spontaneous radiative decay of the upper sublevel is  $A_{ul} = 9.4 \times 10^{-10} \text{ s}^{-1}$  (Sunyaev & Churazov 1984).

In this paper, we evaluate the atomic processes that lead to the production of the hyperfine line in Li-like  $^{57}\text{Fe}$ . We consider direct electron collisional excitation (§ 2.1), proton collisional excitation (§ 2.2), indirect excitation to higher levels followed by radiative cascades (§ 3), and stimulated radiative processes due to the Cosmic Microwave Background Radiation (CMBR) field (§ 4). We present new calculations for the rate of direct electron excitation of the upper hyperfine line (§ 2.1), and for indirect excitation of the 2p sublevels in the same ion, followed by cascade (§ 3.3). We derive the branching ratios for radiative and collisional transitions between the hyperfine sublevels of  $^{57}\text{Fe}$  XXIV (§§ 3.1, 3.2). A total effective collision strength for exciting the line is given in § 3.5. The rate of excitation due resonant scattering of UV and X-ray lines (optical pumping) is discussed in § 3.6. The radiative transfer of the line and of the CMBR is discussed in § 5. The resulting line intensities in a few simple situations are given in § 6, where they are also compared to the line intensities for several EUV and X-ray lines from Fe XXIV. Finally, the results are summarized in § 7. These excitation rates are used to predict the fluxes of this line from clusters in Paper II.

## 2. DIRECT COLLISIONAL EXCITATION

### 2.1. Direct Electron Collisional Excitation

The cross-section for direct electron collisional excitation of the excited hyperfine sublevel is  $\sigma(E) = [\Omega_{lu}/(g_l E)]\pi a_o^2$ , where  $E$  is the colliding electron kinetic energy (in Ryd),  $a_o$  is the Bohr radius, and  $\Omega_{lu}$  is the collision strength. The direct electron collision strength between the hyperfine sublevels was calculated using the distorted wave approximation code developed by Eissner & Seaton (1972). For the Li-like target wavefunctions, the SUPERSTRUCTURE code was used. At the temperatures of interest, the excitation energy of the upper hyperfine sublevel,  $\Delta E_{lu}$ , is very small compared to the kinetic energy of the colliding electron, and the collision is therefore assumed to be elastic.

The reactance matrix elements corresponding to elastic collisions within the  $1s^2 2s$  configuration in LS coupling have been converted to hyperfine structure coupling with  $2 \times 4$  6-j symbols. This method of recoupling is similar to the method used for fine structure reactance matrices (e.g., see the JAJOM program [Saraph 1978]). To avoid confusion, we use the same notation as Saraph (1978). Let  $L_i$ ,  $S_i$ , and  $J_i$  denote the orbital, spin, and total electronic angular momenta, respectively, of the Li-like target ion. Let  $l_i$  and  $s_i = 1/2$  be the orbital and spin angular momenta of the electronic projectile. When we include the nuclear spin  $I = 1/2$ , the total angular momentum of the target ion becomes  $F_i$ , where  $\mathbf{F}_i = \mathbf{J}_i + \mathbf{I}$ . We define the following intermediate couplings:  $\mathbf{K}_i = \mathbf{J}_i + \mathbf{l}_i$  and  $\mathbf{G}_i = \mathbf{F}_i + \mathbf{l}_i$ . The subscripts  $i$  corresponds to any collision channel, while we use  $j$  for the initial channel. During



the collision, the interaction responsible for the transition is the electron-electron electrostatic interaction. The conservation relations for this interaction are  $\mathbf{L} = \mathbf{L}_j + \mathbf{l}_j = \mathbf{L}_i + \mathbf{l}_i$ ,  $\mathbf{S} = \mathbf{S}_j + \mathbf{s}_j = \mathbf{S}_i + \mathbf{s}_i$ , and  $p = p_j = p_i$ , where  $p$  is the parity of the system. Thus, the total electronic angular momentum of the (target + projectile) system,  $\mathbf{J} = \mathbf{L} + \mathbf{S}$ , as well as the total angular momentum including the nuclear spin,  $\mathbf{F} = \mathbf{I} + \mathbf{J}$ , are conserved. The other quantum numbers necessary to define uniquely the target state will be denoted by  $\Gamma_i$ . Using Racah algebra and recoupling of the angular momenta, it is possible to obtain the reactance matrix elements between  $Fp$  channels from the ones between  $SLp$  channels as

$$R^{Fp}(\Gamma_i S_i L_i J_i F_i l_i G_i; \Gamma_j S_j L_j J_j F_j l_j G_j) = \sum_{\substack{S_L J \\ \kappa_i \kappa_j}} C(SLJK_i, S_i L_i J_i F_i l_i G_i) \\ \times R^{SLp}(\Gamma_i S_i L_i l_i; \Gamma_j S_j L_j l_j) C(SLJK_j, S_j L_j J_j F_j l_j G_j), \quad (1)$$

where

$$C(SLJK_i, S_i L_i J_i l_i G_i) = (-1)^a (2K_i + 1) \\ \times [(2S + 1)(2L + 1)(2J_i + 1)(2J + 1)(2G_i + 1)(2F_i + 1)]^{1/2} \\ \times \begin{Bmatrix} I & J_i & F_i \\ l_i & G_i & K_i \end{Bmatrix} \begin{Bmatrix} S_i & L_i & J_i \\ l_i & K_i & L \end{Bmatrix} \begin{Bmatrix} I & K_i & G_i \\ 1/2 & F & J \end{Bmatrix} \begin{Bmatrix} L & S_i & K_i \\ 1/2 & J & S \end{Bmatrix}. \quad (2)$$

The phase factor is  $a = S_i - J_i + K_i - I - F_i - G_i - S - J$ . The collision strengths are obtained directly from the reactance matrices (Saraph 1978).

Figure 1 shows the resulting collision strength for direct electron excitation as function of the kinetic energy of the electron. Note that the collision strength is quite small ( $\Omega_{lu} \approx 10^{-3}$ ) at the energies of interest ( $E \approx 10^2$  Ryd). Direct collisional excitation is weak, in part, because the transition is radiatively forbidden, and the forbidden transition rates drop off rapidly at energies which greatly exceed the excitation energy. As we shall see below, the small collision strength for direct excitation indicates that this is not a very significant process at temperatures of interest. While working on this paper, we received a preprint from Sampson & Zhang (1997) which presented relativistic distorted wave calculations of the collision strength for the same transition. The Sampson & Zhang collision strength is shown as a dashed curve in Figure 1. These calculations are in good agreement with our calculations; the Sampson & Zhang collision strengths are about 7% lower than ours.

The rate of electron collisions which directly excite the hyperfine line per unit volume is  $n_l n_e q_{lu}^{\text{dir}}$ , where  $n_e$  is the electron number density and  $n_l$  is the number density of Li-like  $^{57}\text{Fe}$  in the lower hyperfine sublevel. The rate coefficient is

$$q_{lu}^{\text{dir}} = \frac{8.629 \times 10^{-6} \bar{\Omega}_{lu}(T)}{g_l T^{1/2}} \exp\left(\frac{-\Delta E_{lu}}{kT}\right) \text{ cm}^3 \text{ s}^{-1}. \quad (3)$$

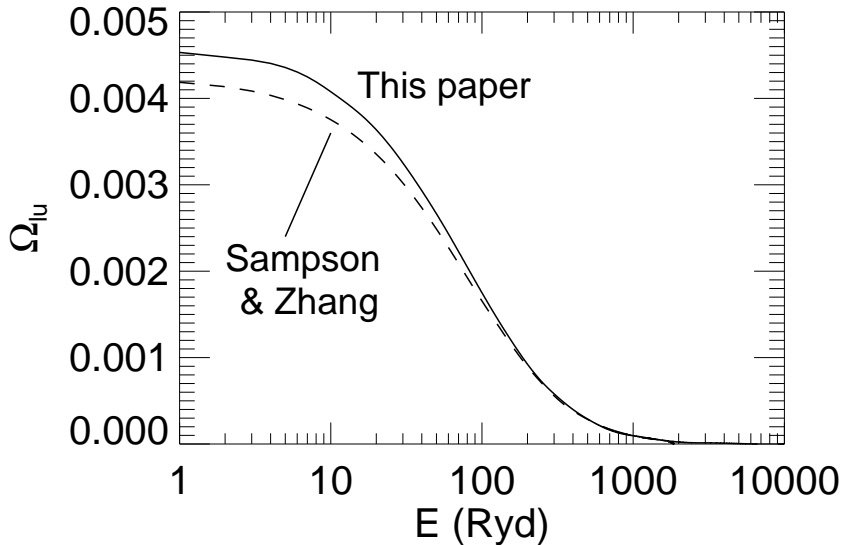


Fig. 1.— strength for direct electron excitation of the hyperfine line as a function of the electron kinetic energy in Rydbergs. The solid curve gives our result, while the dashed line is from Sampson & Zhang (1997).

Here,  $\bar{\Omega}_{lu}(T) \equiv \int_0^\infty \Omega_{lu}(E) \exp(-E/kT) d(E/kT)$ , is the thermally-averaged direct collision strength. The value of  $\bar{\Omega}_{lu}(T)$  as a function of temperature is shown in Figure 2, which is based on the values in Figure 1, for both our calculations and the Sampson & Zhang work. The rate coefficient for de-excitation is related to equation (3) by detailed balance.

## 2.2. Direct Proton Collisional Excitation

Often, proton collisions contribute significantly to the excitation of low-lying energy levels at high temperatures ( $kT \gg \Delta E$ ). This condition clearly applies to the hyperfine sublevels under consideration, but not so strongly to other excited levels in the Fe XXIV ion. Protons are not important for exciting higher levels in Fe XXIV, because they move slower than electrons, undergo Coulomb repulsion, and do not participate in exchange reactions.

The theory of proton collisional excitation was first developed by Seaton (1964), who adapted the theory by Alder et al. (1956) for nuclear Coulomb excitations. Seaton (1964) and Bely & Faucher (1970) used this formalism to calculate the rate of proton collisional excitation of fine structure levels. This theory can also be applied to the excitation of hyperfine transitions. Kastner (1977) and Kastner & Bhatia (1979) give detailed expressions for proton excitation rates based on the theory of Seaton (1964) and Bely & Faucher (1970).

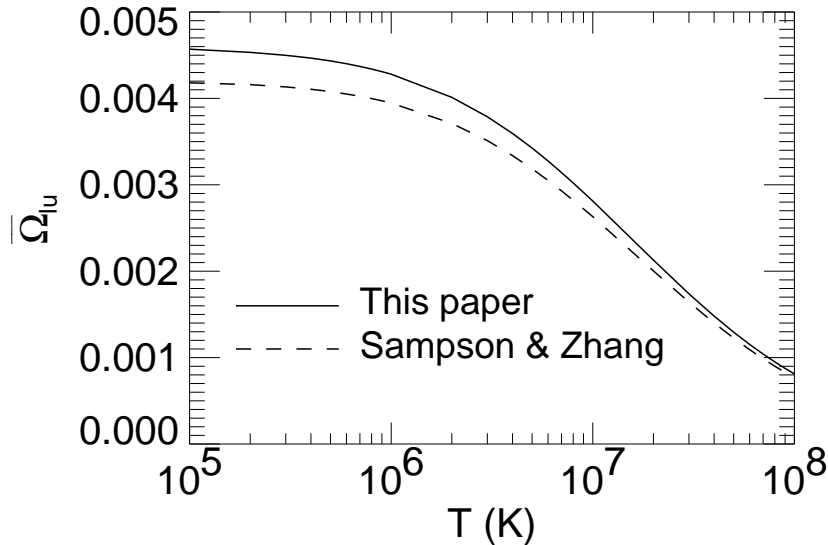


Fig. 2.— Thermally-averaged collision strength for direct electron excitation of the hyperfine line as a function of temperature. The solid curve gives our result, while the dashed line is from Sampson & Zhang (1997).

We applied these expressions to calculate the direct proton excitation of the hyperfine sublevels of the Li-like  $^{57}\text{Fe}$  ion. According to this theory, proton excitations of the fine and hyperfine structure sublevels occur primarily through interactions with the electric quadrupole moment of the ion. For the Li-like ions, the outermost free electron is in the  $2s$  state. Of course, this state is spherically symmetric, and as such has no quadrupole moment. Hence, the dominant term in the rate coefficient for proton excitation is zero.

The next most important term in proton collisional excitation is due to the magnetic dipole interaction. In general, magnetic dipole cross-sections are smaller than electric quadrupole cross-sections by a factor of about  $10^{-5}$  (Alder et al. 1956; Bahcall & Wolf 1968). To check the importance of magnetic dipole excitation rates due to protons, we compared the rate coefficients for this process with that due to electron collisions. The magnetic dipole excitation rates were several orders of magnitude smaller than the electron collision rates. Hence, proton collisions can be neglected.

### 3. INDIRECT COLLISIONAL EXCITATION AND CASCADE

The most important process for exciting the hyperfine line turns out to be electronic collisional excitation to a more highly excited state, followed by radiative cascade to the

excited hyperfine sublevel. We refer to this process as “indirect collisional excitation.” The rate coefficient for excitation of the upper hyperfine sublevel due to excitations of higher levels followed by cascades is given by

$$q_{lu}^{\text{indir}} = \frac{8.629 \times 10^{-6}}{g_l T^{1/2}} \sum_{k>u} C(k, u) \bar{\Omega}_{lk}(T) \exp\left(\frac{-\Delta E_{lk}}{kT}\right) \text{ cm}^3 \text{ s}^{-1}, \quad (4)$$

where the cascade matrix  $C(k, u)$  gives the probability that the radiative decay of level  $k$  will eventually lead to the excitation of the level  $u$ .

In this section, we derive the branching ratios for radiative decays, calculate in detail indirect excitation of the hyperfine line through the  $1s^2 2p$  configuration, give an approximate calculation of the rate of indirect excitations through more highly excited levels, and determine an effective collision strength which gives the total rate of collisional excitation of the hyperfine line.

### 3.1. Radiative Cascades

With the exception of the upper hyperfine sublevel in the ground configuration of  $^{57}\text{Fe}$  XXIV, all of the excited sublevels have allowed radiative decays. Here, we give the branching ratios among the allowed decays between the hyperfine sublevels. We assume LS coupling. Consider the allowed decays between the an upper level with total electron spin  $S$ , total electron orbital angular momentum  $L$ , and total electron angular momentum  $J$ , and a lower level with quantum numbers  $S'$ ,  $L'$ , and  $J'$ . Let the nuclear angular momentum be  $I$ . Let  $A(SLJ, S'L'J')$  be the radiative decay rate between the two levels, averaging over the hyperfine structure (e.g., the value normally given in tables of atomic data). Let  $F$  and  $F'$  be two hyperfine sublevels of the upper and lower levels, respectively. Assume that the hyperfine splittings are small, so that all of the hyperfine transitions have essentially the same wavelength. Then, irreducible tensor analysis can be used to derive the radiative decay rate between the hyperfine sublevels, which is given in terms of a 6-j symbol as

$$A(SLJF, S'L'J'F') = A(SLJ, S'L'J')(2F' + 1)(2J + 1) \left\{ \begin{array}{ccc} J' & J & 1 \\ F & F' & I \end{array} \right\}^2. \quad (5)$$

The nuclear spin of  $^{57}\text{Fe}$  is  $I = 1/2$ . The total decay rate for any given hyperfine sublevel to all of the hyperfine sublevels of a lower level is then

$$\sum_{F'} A(SLJF, S'L'J'F') = A(SLJ, S'L'J'), \quad (6)$$

where this follows from the orthonormality relation for the 6-j symbols. Thus, the total rates of decay of all of the upper hyperfine levels are identical and equal to the rate if the hyperfine structure is not resolved.

Let  $P(nJF, n'J'F')$  be the probability that the excited hyperfine sublevel  $nJF$  decays directly to the hyperfine sublevel  $n'J'F'$ , rather than any other level. Here,  $n$  and  $n'$  represents any other quantum numbers which label the levels. Thus,

$$P(nJF, n'J'F') \equiv \frac{A(nJF, n'J'F')}{\sum_{n'', J'', F''} A(nJF, n''J''F'')}. \quad (7)$$

If one substitutes equation (6) for the decay rate, and simplifies the denominator using the orthonormality relation for 6-j symbols, the decay probability becomes

$$P(nJF, n'J'F') = P(nJ, n'J')(2F' + 1)(2J + 1) \left\{ \begin{array}{ccc} J' & J & 1 \\ F & F' & I \end{array} \right\}^2. \quad (8)$$

Here,  $P(nJ, n'J')$  is the decay probability if the fine structure is not resolved,

$$P(nJ, n'J') \equiv \frac{A(nJ, n'J')}{\sum_{n'', J''} A(nJ, n''J'')}. \quad (9)$$

A very useful quantity in describing indirect collisional excitation and cascades is the cascade matrix  $C(nJF, n'J'F')$ , which is defined as the probability that an excitation of the  $nJF$  hyperfine sublevel leads to a population of the  $n'J'F'$  sublevel by all possible radiative cascade routes. Then, if one starts with the obvious result that  $C(nJF, nJF) = 1$ , one can determine the cascade matrix recursively from the relationship

$$C(nJF, n'J'F') = \sum_{\substack{n, J, F \\ (n'', J'', F'') > (n', J', F')}} C(nJF, n''J''F'') P(n''J''F'', n'J'F'), \quad (10)$$

where the sum extends to all levels above the  $n'J'F'$  sublevel, up to and including the  $nJF$  sublevel. If the upper level  $nJ$  is far above the lower level  $n'J'$ , and there are many intervening levels with allowed decays, and complex cascades dominate the cascade matrix, so that  $C(nJF, n'J'F') \gg P(nJF, n'J'F')$  and  $P(nJF, n'J'F') \ll 1$ , then equation (10) has the approximate solution

$$C(nJF, n'J'F') \approx C(nJ, n'J') \frac{(2F' + 1)}{(2F + 1)} \frac{(2J + 1)}{(2J' + 1)}, \quad (11)$$

where  $C(nJ, n'J')$  is the cascade matrix if the hyperfine structure is not resolved. Thus, complex cascades lead to the populations of hyperfine sublevels  $F'$  in proportion to their statistical weights.

A similar result occurs if the upper hyperfine sublevels  $F$  are populated in proportion to their statistical weights. Then, the average decay probability to the lower hyperfine sublevels  $F'$  is

$$\langle P(nJ, n'J'F') \rangle \equiv \sum_F \frac{(2F+1)}{(2J+1)(2I+1)} P(nJF, n'J'F') = \frac{(2F'+1)}{(2J'+1)(2I+1)} P(nJ, n'J'). \quad (12)$$

Thus, the lower hyperfine sublevels  $F'$  are again populated in proportion to their statistical weights.

The only levels with allowed decays to the ground configuration in Fe XXIV are  $1s^2 np \ ^2P_J$  levels with  $J = 1/2$  or  $3/2$ . The decay probabilities for these hyperfine radiative transitions are listed in Table 1.

Table 1: Hyperfine Radiative Decay Probabilities  $P(JF, J'F')$

Lower Level	Upper Level			
	$J = 1/2$		$J = 3/2$	
	$F = 0$	$F = 1$	$F = 1$	$F = 2$
$F' = 0$	0	1/3	2/3	0
$F' = 1$	1	2/3	1/3	1

### 3.2. Hyperfine Branching Ratios for Electron Collisional Excitation

Collision strengths are available in the literature for excitations to excited levels in Fe XXIV, although these collisional rates average over the hyperfine structure in  $^{57}\text{Fe}$  XXIV. Thus, it is not generally necessary to calculate all of the collision rates anew. Instead, what is needed are the branching ratios for the collisional rates among the hyperfine sublevels. These branching ratios can be determined using irreducible tensor analysis, assuming that the hyperfine structure has a negligible effect on the collision rates. The interaction Hamiltonian between the bound electron and the colliding free electron can be expanded as a power series with terms  $(r_{<}^\lambda/r_{>}^{\lambda+1})$ , where  $\lambda$  is the index of the series, and  $r_{<}$  and  $r_{>}$  are the smaller and larger of the radii of the two interacting electrons. The interactions are further divided into direct interactions (D) in which the bound and free electrons retain their identities, and exchange interactions (E) in which they exchange identities.

For an alkali ion, such as the Li-like system, only the valence electron is strongly affected during the collision. Configuration interactions are negligible between target terms, and only

one  $\lambda$  term contributes to the direct interaction for transitions from the 2s configuration. We can therefore simplify the Racah algebra and reduce the 8 6-j symbols which arise when equation (2) is squared to only 2 6-j symbols. For either direct or exchange reactions, the collision strength for a transition between the hyperfine sublevels is given approximately by

$$\Omega(F, F') = \Omega(J, J')(2F + 1)(2F' + 1) \left\{ \begin{array}{ccc} J' & J & \lambda \\ F & F' & I \end{array} \right\}^2, \quad (13)$$

where  $\Omega(J, J')$  is the collision strength between the fine structure levels, ignoring the hyperfine structure and nuclear spin. An equivalent result has been given by Sampson & Zhang (1997), based on jj coupling. If LS coupling is assumed and the fine structure splitting are also small, then this branching relationship can be extended to include the fine structure in direct interactions as

$$\begin{aligned} \Omega^D(JF, J'F') &= \Omega^D(LS, L'S) \frac{(2J + 1)(2J' + 1)(2F + 1)(2F' + 1)}{(2S + 1)} \\ &\quad \times \left\{ \begin{array}{ccc} L' & L & \lambda \\ J & J' & S \end{array} \right\}^2 \left\{ \begin{array}{ccc} J' & J & \lambda \\ F & F' & I \end{array} \right\}^2. \end{aligned} \quad (14)$$

Here,  $\Omega^D(LS, L'S)$  is the direct collision strength between the two terms, ignoring the fine structure. For direct interactions, the electron spin  $S$  is unchanged.

### 3.3. Indirect Excitation Through 2p Sublevels

In the compilation of collision strengths for Fe XXIV in Gallagher & Pradhan (1985), the largest excitation rates from the 2s ground configuration are to the levels in the low lying 2p configuration. Thus, we treat the 2p sublevels in detail because their collision strengths dominate the excitation of the hyperfine line. These sublevels are shown schematically in Figure 3. The allowed radiative decays and collisional excitation and de-excitation processes are indicated, along with the radiative and collisional branching ratios.

For each of the transitions between 2s and 2p hyperfine sublevels, the collision strength and radiative decay rate (for allowed transitions) were calculated, using the same distorted wave method and recoupling scheme discussed in § 2.1. In Figure 4, we illustrate these values by giving the collision strengths for transitions between the ground hyperfine 2s  $F = 0$  sublevels and the excited 2p hyperfine sublevels. The values are given as a function of the incident electron energy (in Rydbergs) for low energy collision ( $E \leq 50$  Ryd). These results illustrate several points about the collisional excitation.

First, even at these low energies, the collisional excitation is dominated by allowed transitions. Collisional excitations and de-excitations between the 2s  $^2S_{1/2}$   $F = 0$  hyperfine

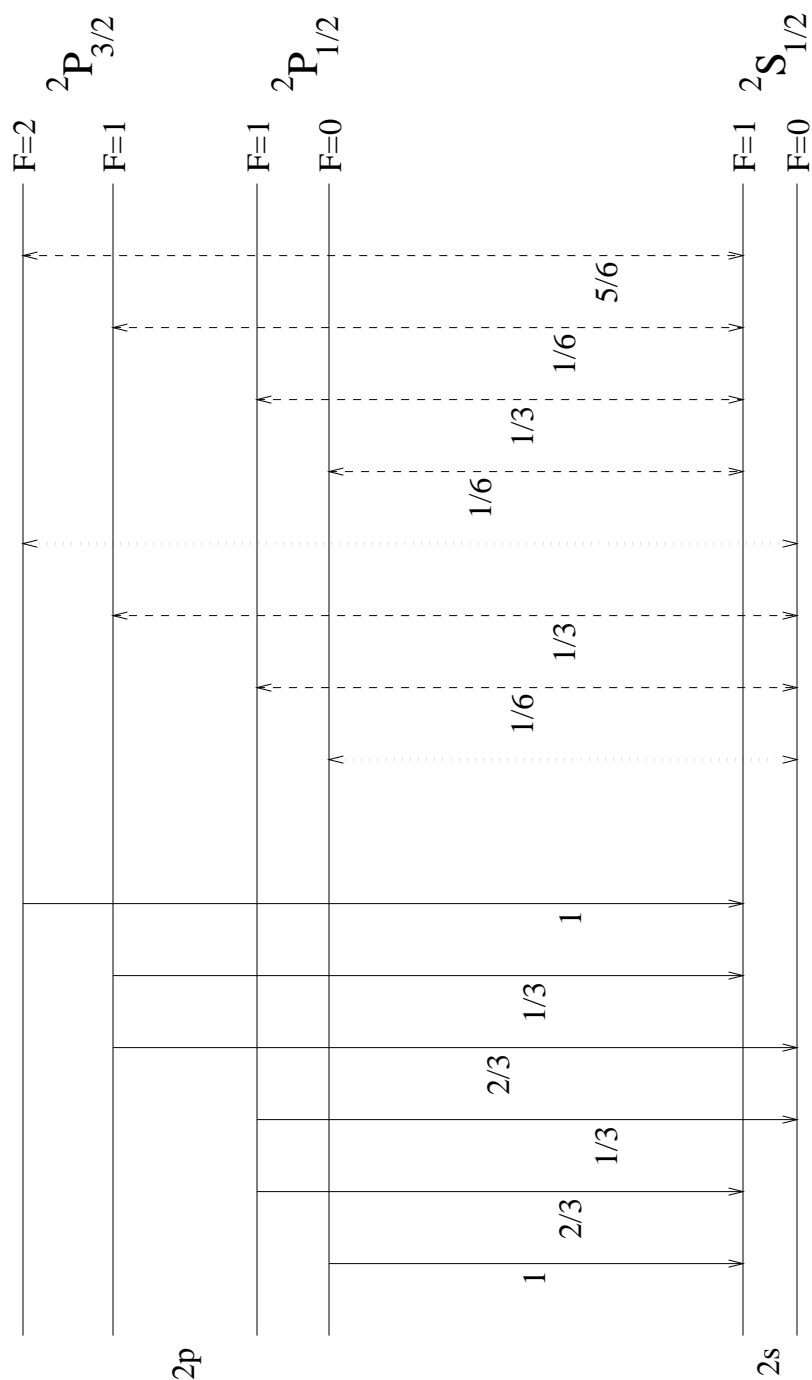


Fig. 3.— A schematic energy level diagram of the 2s and 2p hyperfine levels for  $^{57}\text{Fe XXIV}$ . The energies are not shown to scale. The vertical solid lines on the left show the allowed radiative decays, and the numbers give the branching ratios as defined in Table 1. The vertical lines at the right are the collisional transitions. The dashed lines give the allowed transitions, and the numbers give the branching ratios as defined in Table 2. The dotted lines are the weaker forbidden transitions.



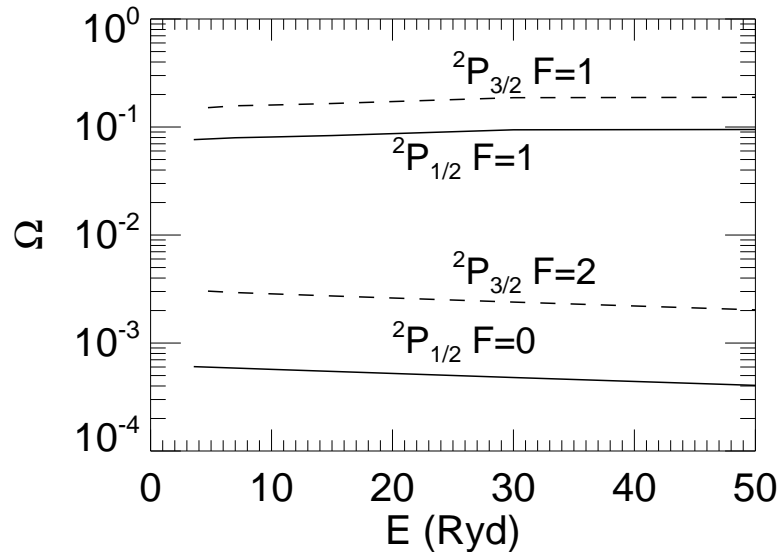


Fig. 4.— Collision strength versus incident electron energy (in Rydbergs) for electron collisions between the ground hyperfine  $2s$   $F = 0$  levels and the excited  $2p$  hyperfine levels of  $^{57}\text{Fe}$  XXIV.

sublevel and the  $2p$   ${}^2P_{1/2}$   $F = 0$  or  ${}^2P_{3/2}$   $F = 2$  hyperfine sublevels are forbidden. In Figure 4, the rates for these forbidden transitions are at least a factor of 20 smaller than the rates for the allowed transitions from the ground  $2s$   ${}^2S_{1/2}$   $F = 0$  hyperfine sublevel to the  $2p$   ${}^2P_{1/2}$   $F = 1$  or  ${}^2P_{3/2}$   $F = 1$  sublevels. When one goes to even higher energies, the allowed transitions dominate even more strongly. In collisional ionization equilibrium, the excitation of the  $^{57}\text{Fe}$  XXIV line should occur mainly at  $E \approx 10^2$  Ryd or  $T \approx 2 \times 10^7$  K (§ 6). This is considerably greater than the threshold for the excitation of the  $2p$   ${}^2P_{1/2}$  or  $2p$   ${}^2P_{3/2}$  levels. Thus, one expects that collisional excitation will be dominated by radiatively allowed transitions. As a result of radiative excitation of the hyperfine ground levels by the cosmic microwave background radiation, the populations of the two hyperfine ground sublevels are expected to be comparable (§ 4). Now, all of the  $2p$  hyperfine sublevels have allowed transitions from either one or both of the ground hyperfine sublevels. Thus, the indirect excitation of the  $^{57}\text{Fe}$  XXIV line through the  $2p$  sublevels will be dominated by allowed electron collisional excitations.

For these allowed electron collisional excitations, the branching ratios are given by equations (13) or (14) with  $\lambda = 1$ . Alternatively, the branching ratios can be found by application of the Van Regemorter (1962) effective Gaunt factor approximation with the radiative branching ratios in Table 1. The branching ratios  $\Omega(F, F')/\Omega(2s, 2p)$  for the collision strengths for the allowed  $2s$  to  $2p$  transitions are given in Table 2, where  $\Omega(2s, 2p)$  is the total collision strength between the two terms (ignoring the nuclear spin). The branching

ratios for allowed collisional excitations are also shown in the left half of Figure 3.

Table 2: Hyperfine Allowed Collisional Branching Ratio  $\Omega(F, F')/\Omega(2s, 2p)$

Lower Level	Upper Level			
	$J = 1/2$		$J = 3/2$	
	$F' = 0$	$F' = 1$	$F' = 1$	$F' = 2$
$F = 0$	0	1/6	1/3	0
$F = 1$	1/6	1/3	1/6	5/6

Second, the collisional excitations and de-excitations between the  $2s\ ^2S_{1/2}\ F = 0$  hyperfine sublevel and the  $2p\ ^2P_{1/2}\ F = 0$  or  $^2P_{3/2}\ F = 2$  hyperfine sublevels are forbidden. As noted above, the collisions have a significantly reduced rate relative to the allowed collision. For forbidden transitions between the singlet  $2s\ F = 0$  hyperfine sublevel and the other sublevels, the collision strength is proportional to the statistical weight of the upper sublevel, so that  $\Omega(2s\ F = 0, 2p\ F = 2)/\Omega(2s\ F = 0, 2p\ F = 0) = 5$ , as shown in Figures 4.

Third, the collisional excitation rates based on our calculations of the collision strength between individual hyperfine sublevels are in excellent agreement ( $\lesssim 7\%$ ) with the values determined by applying the collisional branching ratios (Table 2 or eq. (13)) to the total collision strengths from Hayes (1979). The values in Hayes are the ones used to calculate EUV and X-ray lines from the same ion; as discussed in § 6, these EUV and X-ray lines can be used with the hyperfine line to determine the abundance of  $^{57}\text{Fe}$  accurately. For consistency with with EUV and X-ray analyses of the same plasma, we have adapted the Hayes (1979) collision strengths together with the relevant branching ratios.

### 3.4. Indirect Excitation Through Higher Levels

The collision strengths from the ground configuration to more excited configurations than  $2p$  were obtained from the critical compilation of Gallagher & Pradhan (1985). For most of these transitions, the data come from Hayes (1979). The rest are from Mann (1983). The standard fitting formulae for collision strengths given in Clark et al. (1982) were used to fit the variation of each collision strength with temperature. The collision strength branching ratios of equation (13) were used to partition the collisional excitations among the initial and final hyperfine sublevels. Equations (5) and (10) were used to determine the cascade matrix from the hyperfine sublevels. However, it is worth noting that the collision strengths to higher levels are all at least 30 times smaller than the collision strengths to the  $2p$  levels,

so their contribution is small. Sunyaev & Churazov (1984) first suggested that the dominant line excitation process for this hyperfine line is electron collisional excitation of the 2p levels.

Collisional ionization and recombination also make a small contribution to the overall excitation rate for the hyperfine sublevels. We assume that these processes populate the hyperfine sublevels in proportion to their statistical weights. Note that the cascade matrix among hyperfine sublevels will preserve such a distribution if it is established in the upper sublevels (eq. 12).

### 3.5. *Effective Collision Strength and Resonances*

The collision strengths for direct excitation and indirect excitation of the hyperfine line can be combined to give a single effective collision strength for the transition. By combining equations (3) and (4), one finds

$$\bar{\Omega}_{lu}^{\text{eff}} = \bar{\Omega}_{lu} + \sum_{k>u} \bar{\Omega}_{lk}(T) C(k, u) \exp\left(\frac{-\Delta E_{uk}}{kT}\right). \quad (15)$$

The distorted wave method used to determine the direct collision strength did not include the effect of resonances on the collision rate. Resonances are less important when the incident energy greatly exceeds the excitation energy of the transition. Thus, we do not expect resonances to strongly affect the collisional excitation of the hyperfine line. In collisional excitation through a resonance, the incident free electron and a bound electron form a bound autoionizing state, which autoionizes leaving one bound electron in an excited level. An approximation to the resonance excitation process is to treat each resonance as a direct collisional excitation in which the incoming electron has an energy which is lower than the threshold  $\Delta E_{lk}$  for the excitation (Seaton 1966; Petrini 1970; Mason 1975). The probabilities for the various decay channels of the autoionizing state in the resonance are given by the branching ratios for radiative decay. These same radiative decay probabilities are included in the cascade matrix  $C(k, u)$ . If the resonance structure is assumed to extend down to the level  $u$ , the combined effect of resonances and cascades is given approximately by equation (4), with the excitation energy of the highly excited state replaced by  $\Delta E_{lu}$  (Mason 1975). Thus, we can include resonances approximately by replacing the effective collision strength in equation (15) with

$$\bar{\Omega}_{lu}^{\text{eff}} = \bar{\Omega}_{lu} + \sum_{k>u} \bar{\Omega}_{lk}(T) C(k, u). \quad (16)$$

We use this expression to determine the rate of excitation of the  $^{57}\text{Fe}$  hyperfine line. Since most of the excitation is through the 2p levels, and the excitation energy of these levels is

much less than the temperature at which Fe XXIV is most abundant, this correction for resonances is small.

The resulting values of the effective collision strength as a function of temperature are shown in Figure 5. When the electron collision are dominated by direct excitation and/or allowed collisional excitation followed by direct decay to the ground hyperfine sublevels, the excitation and de-excitation rates obey detailed balance, and the same effective collision strength applies to both excitation and de-excitation. This is the case for the  $^{57}\text{Fe}$  hyperfine line.

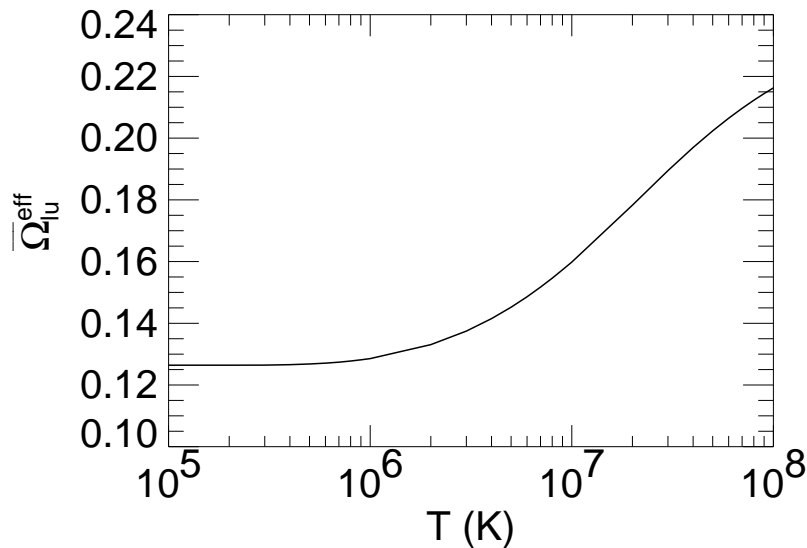


Fig. 5.— Thermally-averaged effective collision strength for excitation and de-excitation of the  $^{57}\text{Fe}$  hyperfine line versus temperature.

### 3.6. *Optical Pumping*

The same indirect electron collisional excitation processes which dominate the collisional excitation of the  $^{57}\text{Fe}$  hyperfine line also produce EUV and X-ray photons. The  $2s - 2p$  excitations produce EUV lines at  $192 \text{ \AA}$  and  $255 \text{ \AA}$ , while the  $2s - 3p$  excitations make an X-ray doublet at  $10.6 \text{ \AA}$ . Photons in these lines, due to the collisional excitation of  $\text{Fe}^{+23}$  or due to some unrelated continuum process, can be absorbed by this ion, and this radiative excitation will normally be followed by a radiative decay. This resonant scattering process can also affect the excitation of the ground hyperfine sublevels through the branching ratios of the radiative cascades to the sublevels (Sunyaev & Churazov 1984). We refer to this

process as “optical pumping.”

Let  $n_l R_{lu}(nSLJ)$  be the rate of excitation per unit volume of ions in the lower ground hyperfine sublevel to the upper ground hyperfine sublevel through the resonant scattering of a line whose upper level is denoted by the quantum numbers  $(nSLJ)$ . Let  $\bar{J}(nSLJ)$  be the line profile averaged mean intensity of this EUV or X-ray line, which is defined by

$$\bar{J}(nSLJ) \equiv \int J_\nu(nSLJ) \phi(\nu) d\nu. \quad (17)$$

Here,  $\phi(\nu)$  is the line profile function, which is normalized so that its integral over all frequencies is unity. The mean intensity of the line,  $J_\nu(nSLJ)$ , is averaged over all directions. Then, it is straightforward to show that

$$R_{lu}(nSLJ) = \left[ \frac{c^2 \bar{J}(nSLJ)}{2h\nu^3} \right] \sum_F \frac{2F+1}{2F_l+1} \frac{A(F, F_l)A(F, F_u)}{\sum_{F'} A(F, F')}, \quad (18)$$

where  $\nu$  is the central frequency of the line,  $F$  denotes a hyperfine sublevel of the upper level  $nSLJ$ , and  $A(F, F')$  is the radiative decay rate of the upper hyperfine sublevel to one of the ground hyperfine sublevels,  $F' = F_l, F_u$ . If one ignores the small difference in  $\bar{J}(nSLJ)$  for the hyperfine components of the line, the symmetrical occurrence of  $F_u$  and  $F_l$  in the radiative decay rate in equation (18) would imply the detailed balance relation  $g_l R_{lu} = g_u R_{ul}$ . When one includes the finite hyperfine splitting of the ground level and treats the line profile in detail including recoil, the relationship for an optically thick line becomes (Field 1959)

$$g_l R_{lu} = g_u R_{ul} \exp\left(\frac{-\Delta E_{lu}}{kT}\right). \quad (19)$$

Equation (18) can be evaluated easily using equations (5) and (6). For any of the important resonance lines in Fe XXIV (2s—2p 192 Å and 255 Å, and 2s—3p 10.6 Å), one finds that

$$R_{lu}(nSLJ) = \frac{2}{3} \left[ \frac{c^2 \bar{J}(nSLJ)}{2h\nu^3} \right] A(nSLJ, 2s \ ^2S_{1/2}), \quad (20)$$

where  $A(nSLJ, 2s \ ^2S_{1/2})$  is the radiative decay rate to the ground level ignoring the hyperfine structure. Thus, the rate of optical pumping is simply related to the total rate of absorption of the line photons.

If the photons being resonantly scattered originated through collisional excitation of  $\text{Fe}^{+23}$ , optical pumping can be thought of as increasing the effective rate of indirect collisional excitation. Crudely, the average rate of collisional excitation will be increased by a factor which is of the order of the optical depth of the line. Under some circumstances, the lines could be moderately optically thick (optical depths  $\lesssim 10^2$ ), and optical pumping might be

quite important (Sunyaev & Churazov 1984). Because of radiative transfer, this is a nonlocal process, which depends on the global structure of the system and on the velocity fields. As a result, we don’t discuss optical pumping any further in this paper. In Paper II, we include optical pumping in determining the excitation of the  $^{57}\text{Fe}$  hyperfine line in clusters of galaxies and cooling flows.

#### 4. LEVEL POPULATIONS AND RADIATIVE EXCITATION

Because the  $^{57}\text{Fe}$  hyperfine line wavelength is near the peak of the Cosmic Microwave Background Radiation (CMBR), it is important to include the stimulated radiative processes as well as spontaneous decay. The rates of stimulated emission and absorption are given by  $B_{ul}\bar{J}$  and  $B_{lu}\bar{J}$ , respectively. The Einstein coefficients  $B_{ul}$  and  $B_{lu}$  are related to the rate for spontaneous decay,  $A_{ul}$ , by the Einstein relations,

$$B_{ul} = \frac{g_l B_{lu}}{g_u} = \frac{c^2}{2h\nu_o^3} A_{ul}, \quad (21)$$

where  $\nu_o = \Delta E_{lu}/h$  is the line-center frequency of the line. The quantity  $\bar{J}$  is the line profile averaged mean intensity of the radiation at the  $^{57}\text{Fe}$  hyperfine line (e.g., eq. [17]).

The CMBR is a blackbody at a temperature of  $T_R = 2.73$  K. Since the hyperfine line wavelength is near the peak of the CMBR, one has to use the Planck function without any approximations. However, the line profile of the hyperfine line is expected to be fairly narrow, and the line profile averaged mean intensity should be given accurately by the blackbody intensity at the line center,  $\bar{J} = B_{\nu_o}(T_R)$ , where  $B_{\nu}(T)$  is the blackbody spectrum.

The time scales for excitation and de-excitation of the 2s hyperfine levels are much shorter than the ages or any other interesting time scales in most astrophysical systems of interest. Thus, we assume that the hyperfine levels are in statistical equilibrium,

$$n_u (A_{ul} + B_{ul}\bar{J} + n_e q_{ul}) = n_l (B_{lu}\bar{J} + n_e q_{lu}). \quad (22)$$

Here,  $n_u$  and  $n_l$  are the number density of ions in the upper and lower hyperfine sublevels, respectively. The total rate coefficient for collisional excitation,  $q_{lu}$ , is determined by replacing the collision strength  $\bar{\Omega}_{lu}$  with the effective collision strength  $\bar{\Omega}_{lu}^{\text{eff}}$  in equation (3). The effective collision strength is given in equation (16) and Figure 5.

The collisional excitation and de-excitation rates are related by detailed balance,

$$q_{lu} = \frac{g_u}{g_l} q_{ul} \exp\left(-\frac{\Delta E_{lu}}{kT}\right). \quad (23)$$

Similarly, the Einstein relations (eq. 21) can be used to substitute for  $B_{lu}$  and  $B_{ul}$  in terms of  $A_{ul}$ . With these simplifications, equation (22) can be solved for the ratio of the occupancy of the upper and lower hyperfine sublevels:

$$\frac{n_u}{n_l} = \frac{g_u}{g_l} \exp\left(-\frac{\Delta E_{lu}}{kT}\right) \left\{ \frac{1 + \left(\frac{A_{ul}}{n_e q_{ul}}\right) \left(\frac{\bar{J}c^2}{2h\nu_o^3}\right) \exp(+\Delta E_{lu}/kT)}{1 + \left(\frac{A_{ul}}{n_e q_{ul}}\right) \left[1 + \left(\frac{\bar{J}c^2}{2h\nu_o^3}\right)\right]} \right\}. \quad (24)$$

The quantity  $[(\bar{J}c^2)/(2h\nu_o^3)]$  is the photon occupation number of the radiation field at the frequency of the line.

The above expression implies that when the electron density is very high, the ratio of level populations approaches LTE at the electron kinetic temperature  $T$ . Given the very small excitation energy  $\Delta E_{lu}$ , this implies that the ratio of level populations approaches that of the statistical weights,  $(n_u/n_l) = 3$ , at high densities. It is useful to define a critical electron density as

$$n_{e,cr} \equiv \frac{A_{ul}}{q_{ul}} \left[ 1 + \left( \frac{\bar{J}c^2}{2h\nu_o^3} \right) \right] \approx 17 \left( \frac{T}{1.8 \times 10^7 \text{ K}} \right)^{1/2} \text{ cm}^{-3}, \quad (25)$$

such that the rates of radiative and collisional de-excitation are equal at this density. The numerical value in equation (25) assumes that the radiation field is the CMBR at a temperature of 2.73 K, and the temperature  $1.8 \times 10^7$  K is the value at which the ionization fraction of  $\text{Fe}^{+23}$  is maximum in collisional ionization equilibrium (see Figure 6). The electron density must be at least this high for the level populations to approach LTE at the electron kinetic temperature. In most astrophysical situations where the  $^{57}\text{Fe}$  line would be produced, the density is considerably less than  $n_{e,cr}$ .

On the other hand, all astrophysical plasmas are immersed in the CMBR. In the limit of very low densities, the level populations due to the CMBR are given by

$$\frac{n_u}{n_l} = \frac{g_u}{g_l} \exp\left(-\frac{\Delta E_{lu}}{kT_R}\right) \approx 0.538. \quad (26)$$

for the temperature of the CMBR in the nearby (i.e., low redshift) universe. Thus, the upper hyperfine level is significantly populated even when there is no collisional excitation.

Because we are most interested in the excitation of the hyperfine line under low density conditions, it is useful to define a small parameter  $\epsilon$  as

$$\epsilon \equiv \frac{n_e}{n_{e,cr}}. \quad (27)$$

Then, in the low density limit, the population is given to first order in  $\epsilon$  as

$$\frac{n_u}{n_l} \approx \frac{g_u}{g_l} \exp\left(-\frac{h\nu_o}{kT_R}\right) \left\{ 1 + \epsilon \left[ \exp\left(\frac{h\nu_o}{kT_R}\right) - 1 \right] \right\}. \quad (28)$$

## 5. RADIATIVE TRANSFER

The emissivity,  $j_\nu$ , and the absorption coefficient,  $\kappa_\nu$ , of the hyperfine line are given by

$$j_\nu = \frac{h\nu}{4\pi} A_{ul} n_u \phi(\nu), \quad (29)$$

and

$$\kappa_\nu = \frac{A_{ul} c^2 \phi(\nu)}{8\pi\nu^2} g_u \frac{n_l}{g_l} \left( 1 - \frac{n_u g_l}{g_u n_l} \right). \quad (30)$$

The source function for the line,  $S$ , is

$$S \equiv \frac{j_\nu}{\kappa_\nu} = \frac{2h\nu_o^3}{c^2} \frac{n_u g_l}{g_u n_l} \left( 1 - \frac{n_u g_l}{g_u n_l} \right)^{-1}. \quad (31)$$

In the low density limit (eq. 28), the source function is approximately

$$S \approx B_{\nu_o}(T_R) \left\{ 1 + \epsilon \left[ \exp\left(\frac{h\nu_o}{kT_R}\right) - 1 \right] \right\}, \quad (32)$$

Typically, the intensity of the line will be much less than that of the CMBR, and we can take  $T_R = 2.73$  K.

For the moment, we will assume that an emission region producing the hyperfine line is homogeneous. Then, the solution of the radiative transfer equation for the intensity,  $I_\nu$ , along any given line-of-sight through the region is

$$I_\nu = I_\nu^o \exp(-\tau_\nu) + S [1 - \exp(-\tau_\nu)], \quad (33)$$

where  $I_\nu^o$  is the incident intensity on the far side of the region. The optical depth is  $\tau_\nu \equiv \int \kappa_\nu ds$ , where  $s$  is the path length along the line-of-sight.

The directly observable quantity is not the brightness of the line, but the difference between the line and the background radiation  $I_\nu^o$ . This difference is

$$\Delta I_\nu \equiv (I_\nu - I_\nu^o) = (S - I_\nu^o) [1 - \exp(-\tau_\nu)]. \quad (34)$$

In most astrophysical environments, the line will be very optically thin,  $\tau_\nu \ll 1$ . Moreover, the background radiation will most often be the CMBR, and the line will be much weaker than the CMBR. Thus, we can take  $I_\nu^o = B_\nu(T_R)$ . All of the  $^{57}\text{Fe}^{+23}$  ions are assumed to be in one of the two hyperfine levels, so that  $n(^{57}\text{Fe}^{+23}) = (n_u + n_l)$ . Then, if the low density expression for the source function (eq. 32) is substituted into equation (34) and the exponential of the optical depth is expanded, the resulting net intensity is

$$\Delta I_\nu = \frac{h\nu_o}{4\pi} D(T_R) \int n_e n(^{57}\text{Fe}^{+23}) q_{lu} \phi(\nu) ds. \quad (35)$$



The correction factor for radiative excitation of the hyperfine structure  $D(T_R)$  is

$$D(T_R) \equiv \frac{1 - \exp(-h\nu_o/kT_R)}{1 + \frac{g_u}{g_l} \exp(-h\nu_o/kT_R)} = 0.533 \text{ for } T_R = 2.73 \text{ K.} \quad (36)$$

Thus, the line intensity is reduced by about a factor of two below that expected if there were no radiative excitation of the levels and all of the electrons were in the lower hyperfine sublevel  $l$ . Note that this factor depends somewhat on the redshift  $z$  of the emitter, since  $T_R = 2.73(1 + z)$ .

For completeness, we note that the hyperfine line intensity in the astrophysically less interesting high density limit ( $n_e \gg n_{e,cr}$ ) is given by

$$\Delta I_\nu = \frac{h\nu_o}{4\pi} \frac{g_u}{g_u + g_l} A_{ul} \int n(^{57}\text{Fe}^{+23}) \phi(\nu) ds, \quad (37)$$

which is equivalent to the expression for the intensity of the 21 cm H I line. The fraction of the ions in the upper hyperfine sublevel (the second factor in eq. [37]) is 3/4, as in hydrogen.

## 6. RESULTING LINE INTENSITIES

We adopted an solar iron abundance of  $\text{Fe}/\text{H} = 4.68 \times 10^{-5}$  by number (Anders & Grevesse 1989). The solar system value of the fraction of iron which is  $^{57}\text{Fe}$  was taken to be 2.3% (Völkening & Papanastassiou 1989). For consistency with the rates of ionization and emission used in many analyses of the X-ray emission of hot plasmas, we used the same atomic physics rates as used in the MEKAL X-ray emission code (e.g., Kaastra et al. 1996), as presented in version 10 of the XSPEC spectral analysis package. The MEKAL program includes some recent improvements in the treatment of the Fe L X-ray lines, including the lines from Fe XXIV (e.g., Liedahl et al. 1995). The ionization and recombination rates in the MEKAL code are basically those from Arnaud & Rothenflug (1985). The ionization fraction of  $\text{Fe}^{+23}$  as a function of temperature is shown in Figure 6.

The luminosity of the hyperfine line in the low density limit can be written as

$$L_{hf} = \Lambda_{hf}(T) \int n_p n_e dV, \quad (38)$$

where the gas is assumed to be isothermal and in collisional ionization equilibrium. The integral is the standard integrated emission measure or emission integral of the plasma, where  $n_p$  is the proton number density and  $V$  is the volume of the gas. The emissivity coefficient  $\Lambda_{hf}(T)$  is shown in Figure 7 for solar abundances; it is proportional to the abundance of  $^{57}\text{Fe}$ . In calculating the values in Figure 7, we included ionization and recombination in the

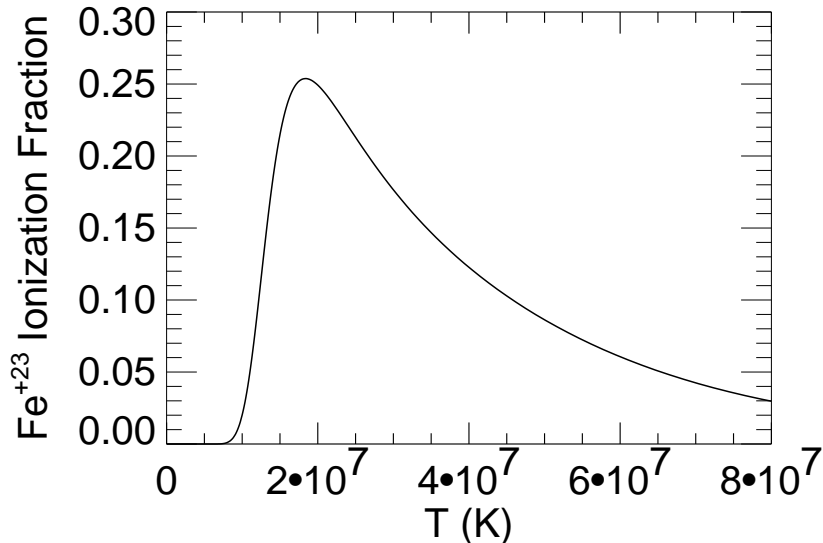


Fig. 6.— The ionization fraction of  $\text{Fe}^{+23}$  as a function of temperature. The ionization fraction peaks at a temperature of about  $1.8 \times 10^7$  K.

line excitation. By comparing Figures 6 and 7, it is clear that the temperature dependence of the emissivity coefficient is mainly due to the variation of the ionization fraction of  $\text{Fe}^{+23}$  with temperature. The emissivity coefficient peaks around  $1.8 \times 10^7$  K.

In the paper which originally suggested that the  $^{57}\text{Fe}$  line might be of astrophysical interest, Sunyaev & Churazov (1984) estimated the excitation rate of the  $^{57}\text{Fe}$  line along with many other hyperfine lines. For fixed abundances and ionization fractions, their estimate of the line excitation rate is about a factor of three higher than our values. They estimated that one-half of all excitations of the 2p levels lead to excitations of the upper hyperfine level. The actual ratio is slightly lower (4/9 at high energies; see Tables 1 and 2). The primary difference would seem to be that their values for the 2s–2p excitation rates are about a factor of three higher than ours. There is some ambiguity in their paper between the definitions of excitation and de-excitation rates, and their expression for the excitation rate may have an extra factor of  $(g_u/g_l)$ . This could account for the difference in excitation rates. When it comes to determining the emissivity of the gas at a given temperature, their values exceed ours by a larger factor, because of the assumption of a higher peak ionization fraction for  $\text{Fe}^{+23}$ . On the other hand, their adopted solar abundance for  $^{57}\text{Fe}$  is slightly lower than ours. In any case, it is clear that the intent of the Sunyaev & Churazov paper was only to give crude estimates of the intensities of a large number of hyperfine lines to support the suggestion that they might be observable.

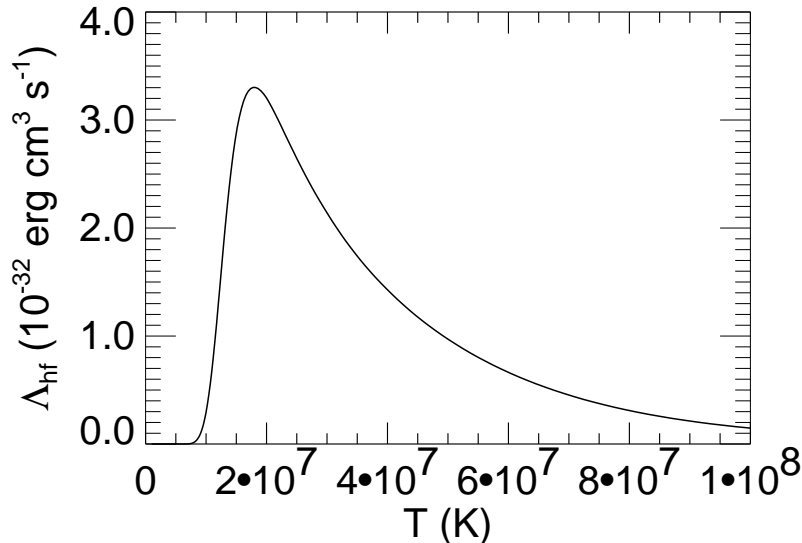


Fig. 7.— The emissivity coefficient  $\Lambda_{hf}(T)$  of the  $^{57}\text{Fe}^{+23}$  hyperfine line as a function of temperature, assuming solar abundances and collisional ionization equilibrium. The temperature dependence is mainly due to the ionization fraction of  $\text{Fe}^{+23}$  and hence peaks at a temperature of  $1.8 \times 10^7$  K.

We also calculated the emission of the hyperfine line in a plasma cooling isobarically due to its own radiation, in the low density limit. The luminosity of the hyperfine line in gas cooling from a temperature  $T$  is given by (White & Sarazin 1987)

$$L_{hf} = \dot{M} \left[ \frac{5}{2} \frac{k}{\mu m_H} \int_0^T \frac{\Lambda_{hf}(T')}{\Lambda(T')} dT' \right] = \Gamma_{hf}(T) \dot{M}, \quad (39)$$

where  $\Lambda_{hf}(T)$  is the emissivity coefficient of the hyperfine line,  $\Lambda(T)$  is the coefficient for the total emissivity of the gas (also sometimes called the cooling function),  $\mu$  is the mass per particle in the gas in units of the mass of the hydrogen atom  $m_H$ , and  $\dot{M}$  is the rate at which gas is cooling (in  $\text{g s}^{-1}$ ). The function  $\Gamma_{hf}(T)$  is defined by the quantity in brackets in equation (39), and is given in Figure 8.  $\Gamma_{hf}(T)$  gives the emission per unit mass of cooling gas, as a function of the initial temperature of the gas. Again, we used the cooling function derived from the MEKAL code as presented in XSPEC (version 10). Solar abundances are used in computing the luminosity. The value of  $\Gamma_{hf}$  rises rapidly with temperature through the value at which the  $\text{Fe}^{+23}$  ion is most abundant,  $1.8 \times 10^7$  K. At temperatures greater than about  $7 \times 10^7$  K, the value of  $\Gamma_{hf}$  flattens out, since all gas which starts at higher temperature passes completely through the temperature range where the line is emitted strongly.

For the purpose of determining the fraction of iron which is  $^{57}\text{Fe}$ , it is more useful to compare the strength of the hyperfine line to other iron lines. In particular, if the comparison

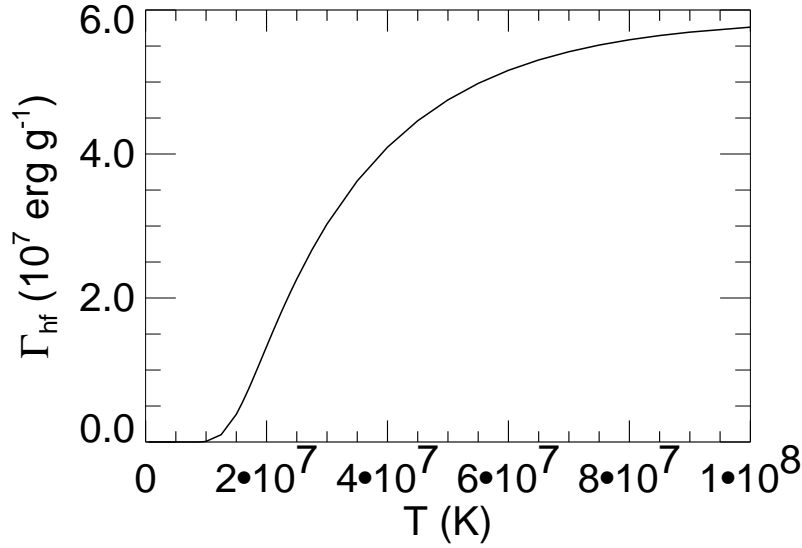


Fig. 8.— The emission of the  $^{57}\text{Fe}^{+23}$  hyperfine line from a gas cooling isobarically subject to its own radiation. The function  $\Gamma_{hf}(T)$  gives the energy radiated per unit mass of cooling gas, as a function of the initial temperature of the gas (eq. 39). Solar abundances and collisional ionization equilibrium are assumed.

is made to lines produced by the same ion  $\text{Fe}^{+23}$ , then the derived fractional abundance of  $^{57}\text{Fe}$  is nearly independent of the ionization structure in the gas. On the other hand, the absolute flux of the hyperfine line is very strongly affected by the ionization structure, as is seen in Fig. 7.

In principle, the best lines for this purpose are the  $\text{Fe}^{+23}$   $2s - 2p$  lines, which are  $2s\ ^2\text{S}_{1/2} - 2p\ ^2\text{P}_{3/2}$  192.02 Å and  $2s\ ^2\text{S}_{1/2} - 2p\ ^2\text{P}_{1/2}$  255.10 Å. These lines are excited by same collisional excitations which we have found to be the main excitation source for the  $\text{Fe}^{+23}$  hyperfine line. As a result, the ratio of the luminosity of the hyperfine line to the luminosity of either of these two extreme ultraviolet (EUV) lines is nearly independent of the temperature or ionization state of the gas. To the extent that the excitation of the hyperfine line is dominated by  $2s-2p$  collisional excitations, the line ratios depend mainly on the wavelengths of the lines, the fractional abundance of  $\text{Fe}^{+23}$ , the radiative correction factor  $D(T_R)$  (eq. 36), and the branching ratios (Table 2). For example, in the limit where  $2s-2p$  excitations dominate the hyperfine line and the temperature is much greater than the excitation energy of these transitions, the luminosity ratio to the  $2s\ ^2\text{S}_{1/2} - 2p\ ^2\text{P}_{3/2}$  192.02 Å line is

$$\frac{L(hf)}{L(192\text{Å})} \approx \frac{2}{3} D(T_R) \left( \frac{192\text{Å}}{3.071\text{mm}} \right) \left[ \frac{n(^{57}\text{Fe})}{n(\text{Fe})} \right] \approx 2.2 \times 10^{-6} \left[ \frac{n(^{57}\text{Fe})}{n(\text{Fe})} \right]. \quad (40)$$

The term in brackets is the relative abundance of  $^{57}\text{Fe}$ . The equivalent result for the other EUV line ( $2s\ ^2S_{1/2} - 2p\ ^2P_{1/2}$  255.10 Å) is

$$\frac{L(hf)}{L(255\text{Å})} \approx \frac{4}{3} D(T_R) \left( \frac{255\text{Å}}{3.071\text{mm}} \right) \left[ \frac{n(^{57}\text{Fe})}{n(\text{Fe})} \right] \approx 5.9 \times 10^{-6} \left[ \frac{n(^{57}\text{Fe})}{n(\text{Fe})} \right]. \quad (41)$$

In Figure 9, the  $L(hf)/L(192\text{Å})$  line ratio is given from a more detailed calculation including all excitation processes for both lines, and assuming the solar isotope fraction of  $^{57}\text{Fe}$  of 2.3%. The 192 Å line was calculated using the MEKAL code. Other excitation processes produce a slight temperature variation and increase the line ratio by about 20% above the analytical estimate at about 120 Ryd. As the temperature increases above  $2 \times 10^7$  K, the ionization fraction of  $\text{Fe}^{+23}$  decreases (Figure 6), and recombination from  $\text{Fe}^{+24}$  to  $\text{Fe}^{+23}$  becomes an important excitation process for both the hyperfine line and the 192 Å line. This causes the increase in the line ratio at high temperatures as seen in Figure 9.

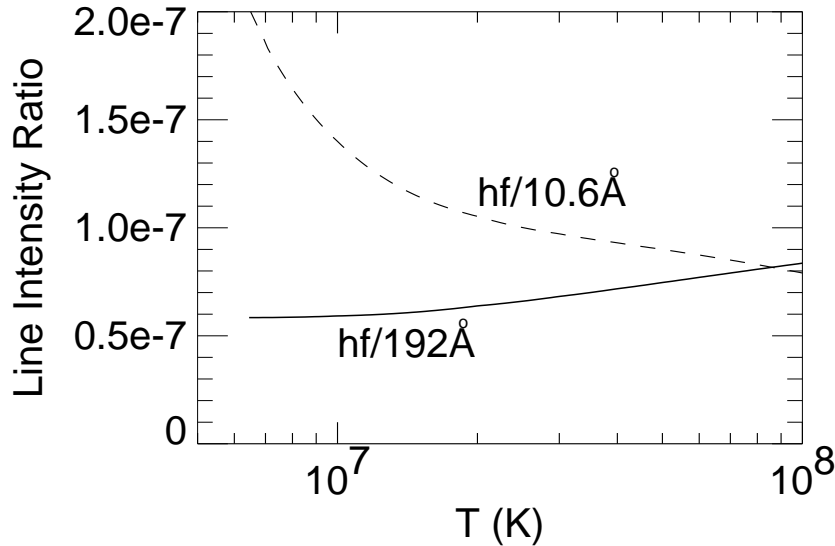


Fig. 9.— The ratios of the luminosity of the  $^{57}\text{Fe}^{+23}$  hyperfine line to the strongest EUV and X-ray lines from  $\text{Fe}^{+23}$ . The solid curve is the ratio to the EUV line  $2s\ ^2S_{1/2} - 2p\ ^2P_{3/2}$  192.02 Å line, while the dashed curve is the ratio to the  $2s\ ^2S_{1/2} - 3p\ ^2P_{1/2,3/2}$  10.663, 10.619 Å doublet.

One negative feature of the 2s—2p EUV lines is that they are in a part of the spectrum which is difficult to observe, partly because of Galactic absorption. Moreover, their fluxes might be uncertain even if detected because of the correction for absorption. The 2s—3p X-ray lines from  $\text{Fe}^{+23}$  are easier to observe, and less subject to absorption. An alternative standard of comparison might be the allowed doublet of 2s—3p lines,  $2s\ ^2S_{1/2} - 3p\ ^2P_{3/2}$

10.619 Å and  $2s\ ^2S_{1/2} - 3p\ ^2P_{1/2}$  10.663 Å. Because this doublet is difficult to resolve, we consider the luminosity  $L(10.6\ \text{Å})$  of the sum of the two lines. The ratio of the hyperfine line to this doublet is also shown in Figure 9. The 10.6 Å line was calculated using the MEKAL code. Due to the higher excitation energy of this doublet and the difference in the temperature dependence of the collision strengths exciting the hyperfine line and the  $2s-3p$  X-ray doublet, this line ratio is much more temperature dependent.

The observability of this line is crucially dependent on its wavelength. We use a wavelength value of 3.071 mm from the paper by Shabaeva & Shabaev (1992). The uncertainty in this number is about 0.15% (Shabaev, Shabaeva & Tupitsyn 1995), which translates into a velocity uncertainty of about 450 km s<sup>-1</sup>. This is larger than the bandwidth of many radio spectrometers in this wavelength region. On the other hand, the widths of the <sup>57</sup>Fe lines expected in astrophysical environments may well be even broader (e.g., Paper II). Hence undertaking observations of this line will be difficult unless a spectrometer with a large bandwidth is used. We will discuss the detectability of this line further in Paper II.

## 7. SUMMARY

Sunyaev & Churazov (1984) first showed that the 3.071 mm hyperfine line from Li-like <sup>57</sup>Fe might be observable in astrophysical plasmas. We have assessed the various atomic processes that can contribute to the excitation of this line. We calculated the rate of direct electron collisional excitation of the upper hyperfine level, and found it to be small. The rate of proton collisional excitation was shown to be negligible. We calculate the rate of excitation of the line by electron collisional excitation of more highly excited states, followed by radiative cascade. We derive the branching ratios for allowed radiative decays to different hyperfine sublevels, and the resulting cascade matrix. We also derive branching ratios for the electron collisional excitation of hyperfine sublevels for direct and exchange interactions.

As originally suggested by Sunyaev & Churazov (1984), the dominant process in the excitation of the 3.071 mm hyperfine line is electron collisional excitation of the 2p levels, followed by cascade. We calculate the excitation rates for this process, and show that they are dominated by radiatively allowed transitions, for which the collision strengths can be derived easily from existing calculations of the collision strengths and the branching ratios. We derive an effective collision strength for exciting the hyperfine line which includes the direct collisional excitation, the excitation of the 2p levels and higher levels, cascades, and a correction for resonances.

At the wavelength of the 3.071 mm hyperfine line, induced radiative transitions due

to the Cosmic Microwave Background Radiation (and possibly, other microwave radiation sources) are important. We calculate the effect of the CMBR on the level populations and line excitation. We determine the net intensity of the line above the background radiation. The plasmas that radiate the hyperfine line will most likely have electron densities that are much lower than the electron densities at which radiative decays and collisional excitation are balanced. Thus, we derive expressions for the net line intensity in this low density limit.

We determine the intensity of the hyperfine line from an isothermal, coronal plasma in collisional ionization equilibrium with solar abundances. Because collisional excitation of the line varies slowly with  $T$  is mainly due to the variation in the ionization fraction of  $\text{Fe}^{+23}$ . For a given emission measure, the line intensity is maximum at a temperature of about  $1.8 \times 10^7$  K. Our emission rates are somewhat smaller than the estimates given by Sunyaev & Churazov (1984). We have also derived the hyperfine line luminosity emitted by a coronal plasma cooling isobarically due to its own radiation.

Because of the strong dependence of the hyperfine line emissivity on the ionization state of the gas, the isotopic abundance of  $^{57}\text{Fe}$  relative to the total iron abundance is best determined by comparing the hyperfine line to other lines emitted by the same ion,  $\text{Fe}^{+23}$ . We suggest that ratios to the 2s—2p EUV lines at 192 Å and 255 Å or the 2s—3p X-ray lines at 10.6 Å be used to derive isotopic abundances. We derive these line ratios as a function of temperature.

In Paper II, we will apply these results to predict the properties of the 3.071 mm  $^{57}\text{Fe}^{+23}$  hyperfine line from cooling flow and non-cooling flow clusters of galaxies.

**Acknowledgements** C. L. S. was supported in part by NASA Astrophysical Theory Program grant 5-3057. We thank Bob Brown, Eugene Churazov, Dave Frayer, and Rashid Sunyaev for useful comments. We thank Doug Sampson for sending up his results in advance of publication.

## REFERENCES

- Alder, K., Bohr, A., Huus, T., Mottleson, B., & Winther, A. 1956, *Rev. Mod. Phys.*, 28, 432  
 Anders, E., & Grevesse, N. 1989, *Geochim. Cosmochim. Acta*, 53, 197  
 Arnaud, M., & Rothenflug, M. 1985, *A&AS*, 60, 425  
 Bahcall, J. N., & Wolf, R. A. 1968, *ApJ*, 152, 701  
 Balser, D. S., Bania, T. M., Rood, R. T., & Wilson, T. L. 1997, *ApJ*, 483, 320  
 Bely, O., & Faucher, P. 1970, *A&A*, 6, 88  
 Clark, R. E. H., Magee, Jr., N. H., Mann, J. B., & Merts, A. L. 1982, *ApJ*, 254, 412  
 D’Cruz, N. L., & Sarazin, C. L. 1998, in preparation (Paper II)  
 Dickey, J. M., & Lockman, F. J. 1990, *ARA&A*, 28, 215  
 Eissner & Seaton, M. J. 1972, *J. Phys. B*, 5, 2187

- Field, G. B. 1959, *ApJ*, 129, 551
- Gallagher, J. W., & Pradhan, A. K. 1985, An Evaluated Compilation of Data for Electron-Impact Excitation of Atomic Ions, JILA Information Center Rept. No. 30 (Boulder: University of Colorado), 172
- Hayes, M. A. 1979, *MNRAS*, 189, 49p
- Kaastra, J. S., Mewe, R., Liedahl, D. A., Singh, K. P., White, N. E., & Drake, S. A. 1996, *A&A*, 314, 547
- Kastner, S. O. 1977, *A&A*, 54, 255
- Kastner, S. O., & Bhatia, A. K. 1979, *A&A*, 71, 211
- Liedahl, D. A., Osterheld, A. L., & Goldstein, W. H. 1995, *ApJ*, 438, L115
- Lubowich, D. A., Anantharamiah, K. R., & Pasachoff, J. M. 1989 *ApJ*, 345, 770
- Mann, J. B. 1983, *At. Data Nucl. Data Tables*, 29, 407
- Mason, H. E. 1975, *MNRAS*, 170, 651
- Petrini, D. 1970, *A&A*, 9, 392
- Rood, R. T., Bania, T. M., Wilson, T. L., & Balsler, D. S. 1995, in *ESO/EIPC Workshop on the Light Elements*, ed. P. Crane (Heidelberg: Springer), 201
- Sampson, D. H., & Zhang, H. L. 1997, *J. Phys. B: At. Mol. Opt. Phys.*, 30, 28
- Saraph, H. E. 1978, *Comp. Phys. Comm.*, 15, 247
- Seaton, M. J. 1964, *MNRAS*, 127, 191
- Seaton, M. J. 1966, *Proc. Physical Soc.*, 88, 801
- Shabaeva, M. B., & Shabaev, V. M. 1992, *Phys. Lett. A*, 165, 72
- Shabaev, V. M., Shabaeva, M. B. & Tupitsyn, I. I. 1995, *Phys. Rev. A*, 52, 3686
- Sunyaev, R. A., & Churazov, E. M. 1984, *Soviet Ast. Lett.*, 10, 201
- Van Regemorter, H. 1962, *ApJ*, 136, 906
- Völkening, J., & Papanastassiou, D. A. 1989, *ApJ*, 347, L43
- White, R. E., & Sarazin, C. L. 1987, *ApJ*, 318, 621